Overview of Wireless Power Conversion Technologies Topology, Modulation, and Control

Kerui Li[1] and Jialong Qu[2]

1 School of Electrical and Electronics Engineering, Nanyang Technological University, Singapore

2 Energy Research Institute @ NTU, Nanyang Technological University, Singapore

Part A: New Challenges to the Stability of Wireless Power Transfer System

Outline

- Motivation
- Challenge: Beat frequency oscillation
  - Solutions:
    - Hybrid topology
    - Modulation
- Challenge: Right-half-plane zeros
  - Solutions:
    - Control methods for alleviating the adverse effects of right-half-plane zeros
    - Control methods for eliminating the right-half-plane zeros

Wireless power transfer

- The market of wireless power devices is fast growing (double-digit growth)
- Advanced wireless power conversion technologies are needed

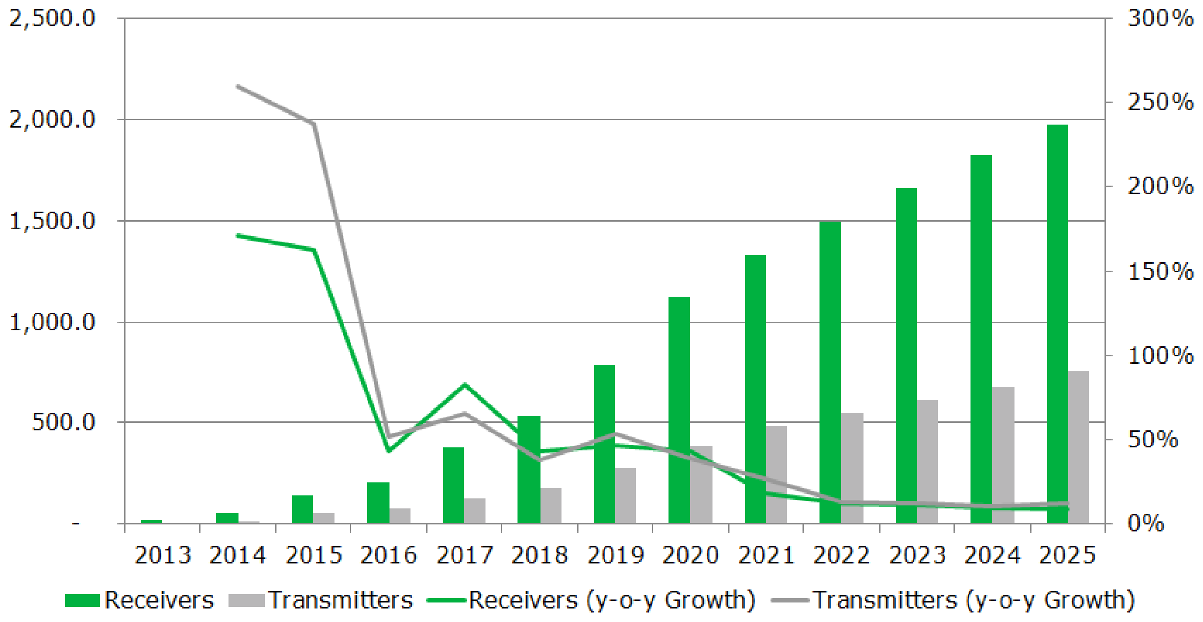

Source: IHS Markit

[1] M. Markides, V. Fodale, and D. Kithany, “Wireless Power Market Tracker”, IHS Markit.

Wireless power transfer

- Wireless power standards are still evolving
  - Higher power
    - Consumer electronics (increase to 120 W) [1]
    - Heating appliances (increase to 2.2 kW) [2]
    - Electric vehicle (increase to 200 kW) [3]
    - …
  - More applications
    - Batteryless drones
    - Waterproof outdoor robots
    - Vehicle to grid (V2G)
    - …

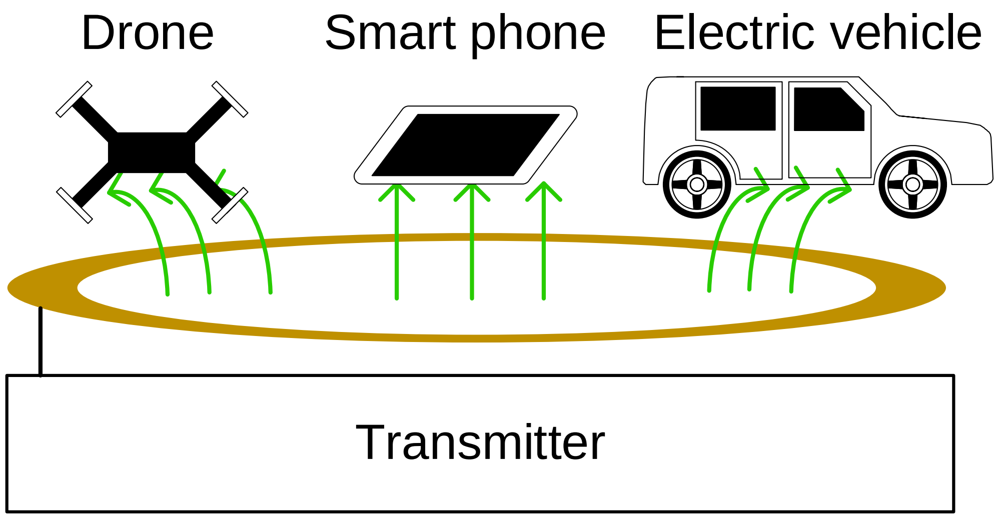

[1] C. K. Michael Tse, "Short course on wireless power transfer technologies," Hong Kong, 2019
[2] Wireless Power Consortium, "Ki cordless kitchen: from concept to industry standard," 2019
[3] SAE Standard, "Wireless power transfer for light-duty plug-in/electric vehicles and alignment methodology," 2017

Background and Motivation

- Wireless power transfer provides a convenient and safe method for charging.
- The market potential is huge and fast-growing (Devices shipment: **2 billion units** in 2025 [1])

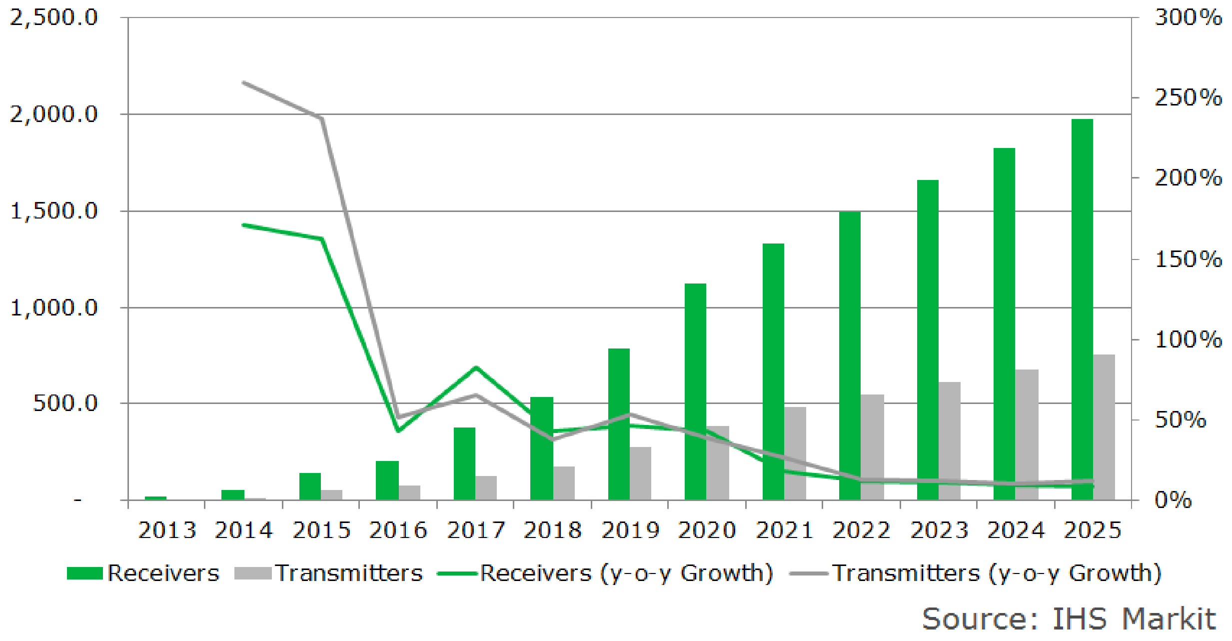

[1] M. Markides, V. Fodale, and D. Kithany, "Wireless Power Market Tracker", IHS Markit.

Background and Motivation

- **Higher power**
  - From a few watts to tens of kilowatts
- **Higher robustness**
  - From stationary charging to dynamic charging
- **Higher stability**
  - From indoor to outdoor

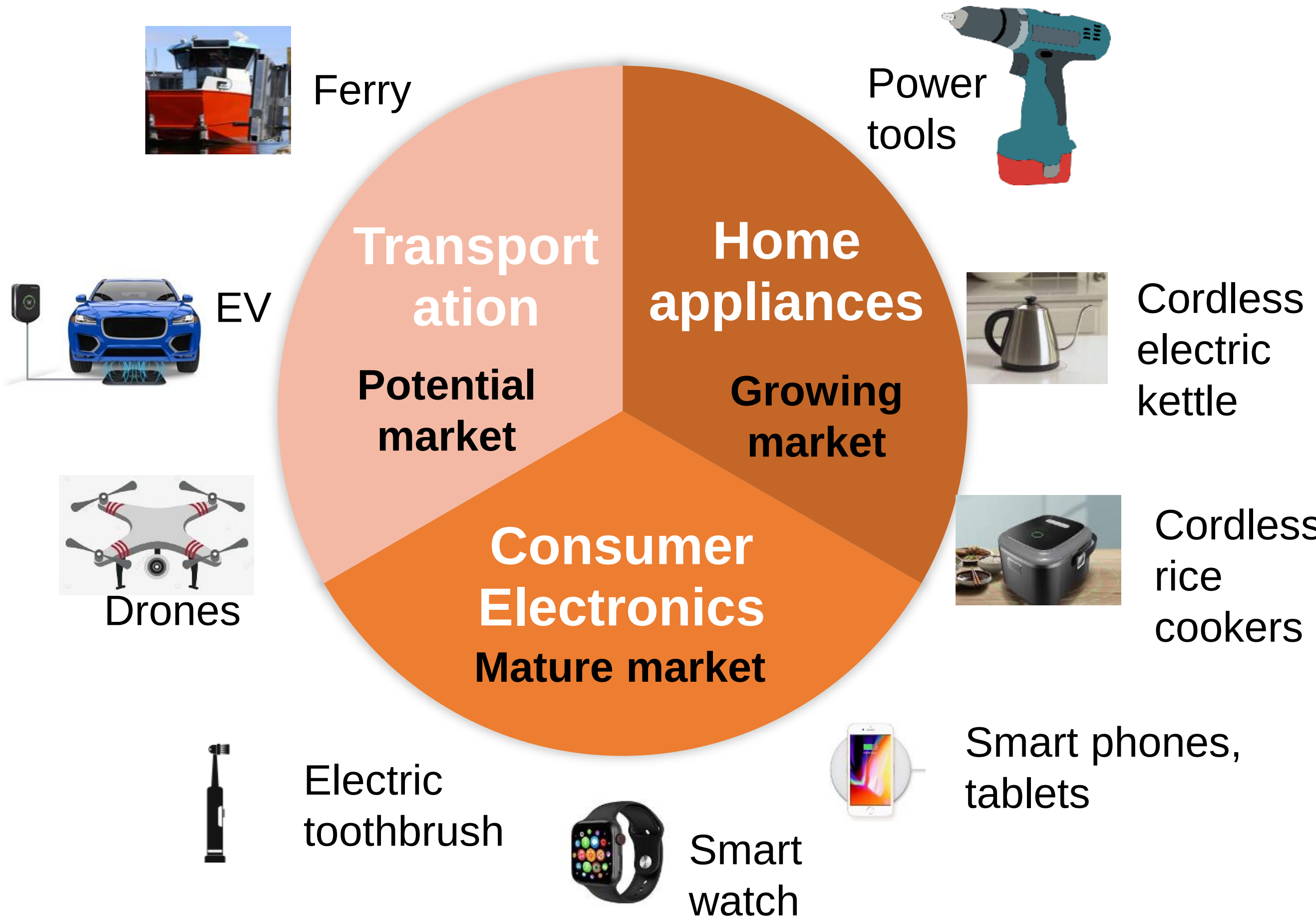

Wireless power transfer

- Wireless power transmission
  - How to transmit and receive AC over the air?

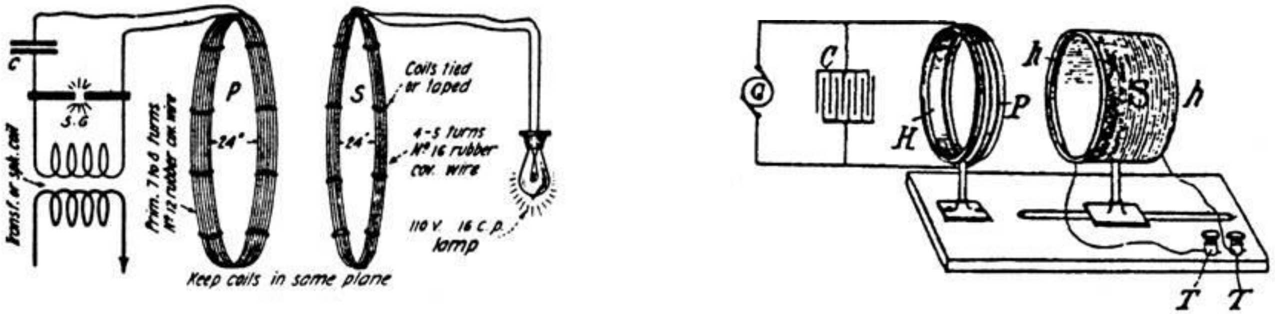

Nikola Tesla's inventions

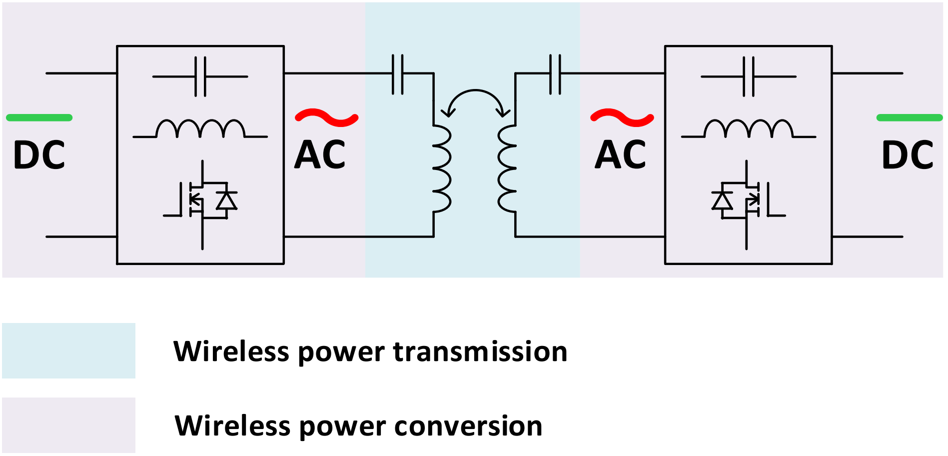

- Wireless power conversion
  - How to effectively and efficiently covert DC to high-frequency AC and vice versa?

[1] N. Tesla, "High frequency oscillators for electro-therapeutic and other purposes," Proceedings of the IEEE, vol. 87, no. 7, p. 1282, 1999
[2] S. Y. Hui, "Planar wireless charging technology for portable electronic products and Qi," Proceedings of the IEEE, vol. 101, no. 6, pp. 1290–1301, 2013

Outline

- Motivation
- Challenge: Beat frequency oscillation
  - Solutions:
    - Hybrid topology
    - Modulation
- Challenge: Right-half-plane zeros
  - Solutions:
    - Control methods for alleviating the adverse effects of right-half-plane zeros
    - Control methods for eliminating the right-half-plane zeros

Existing solution

Reference design of wireless power standard [1]

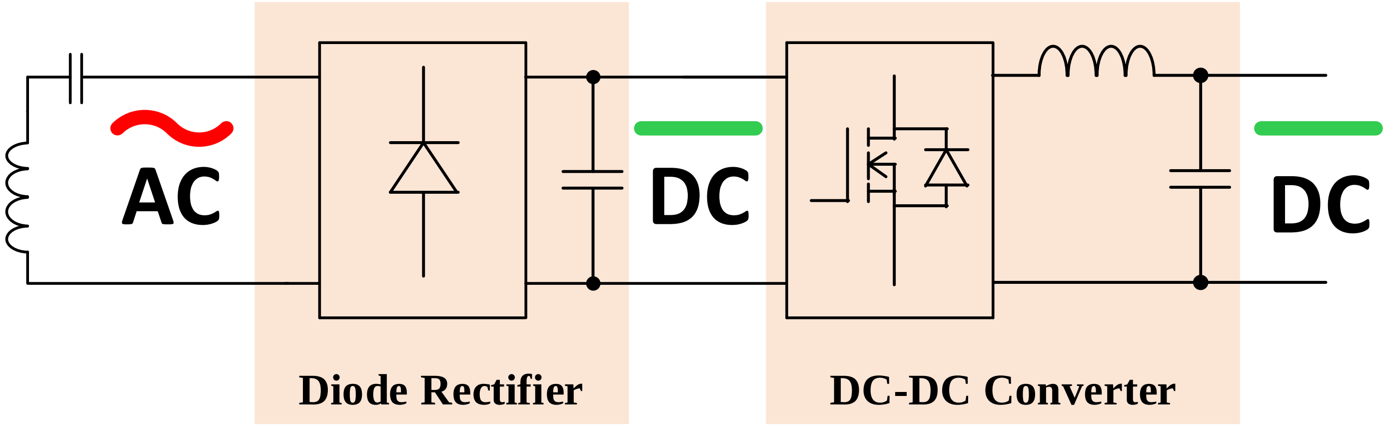

- Functionality:
  - Diode rectifier – AC to DC conversion, unregulated DC
  - DC-DC converter – DC to DC conversion, regulated DC
- Features:
  - Simple circuit structure
  - Ease of implementation

[1] The Qi wireless power transfer system power class 0 specification Part 4: reference designs, Wireless power consortium, Feb. 2017

Challenges

Beat frequency oscillation

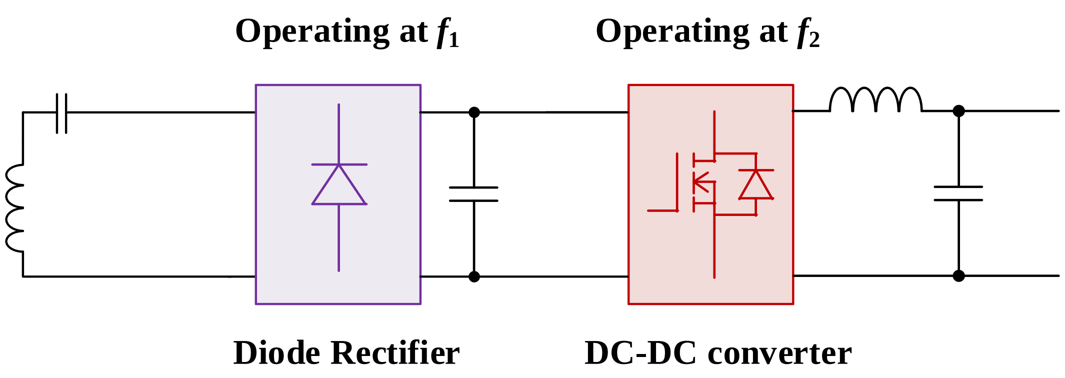

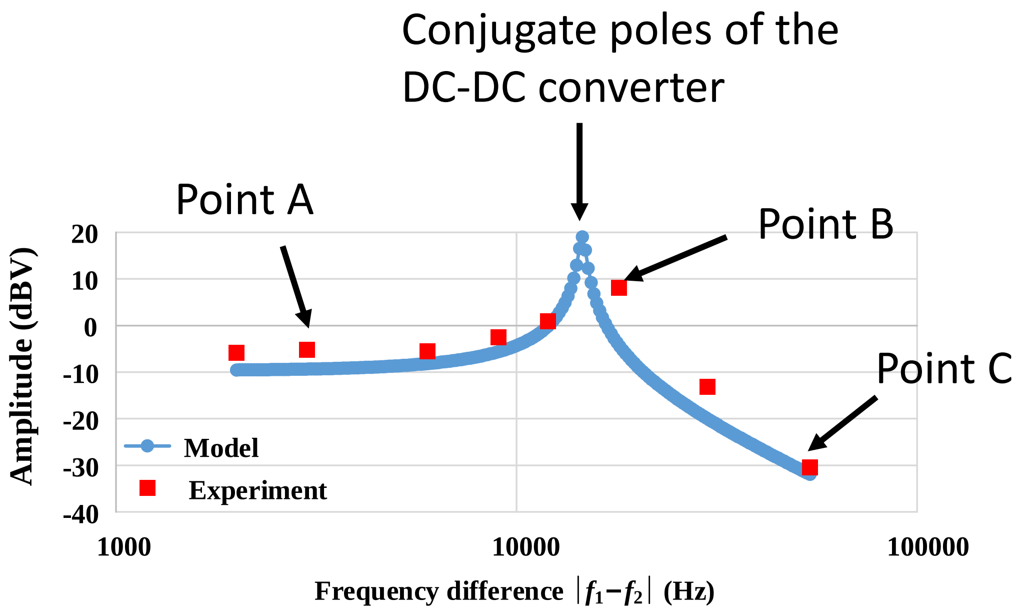

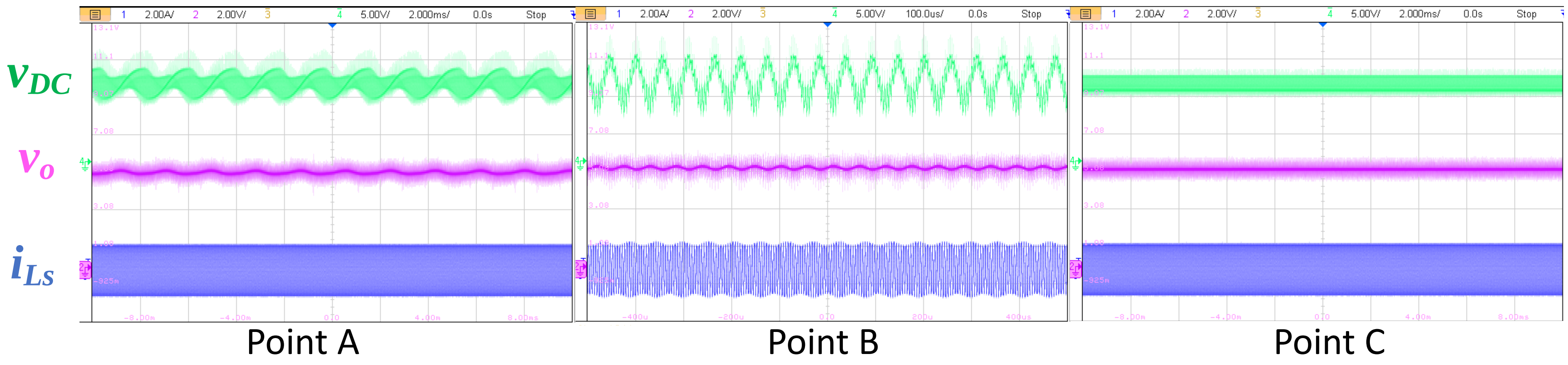

- Identify a new instability factor
- Model the oscillation quantitatively

[1] **K. Li**, S. C. Tan and S. Y. R. Hui, "On Beat Frequency Oscillation of Two-Stage Wireless Power Receivers", IEEE Transactions on Power Electronics, vol. 35, no. 12, pp. 12741-12751, Dec. 2020.

Challenges

How to eliminate the beat frequency oscillation?

- Frequency Synchronization ($f_1 = f_2$)

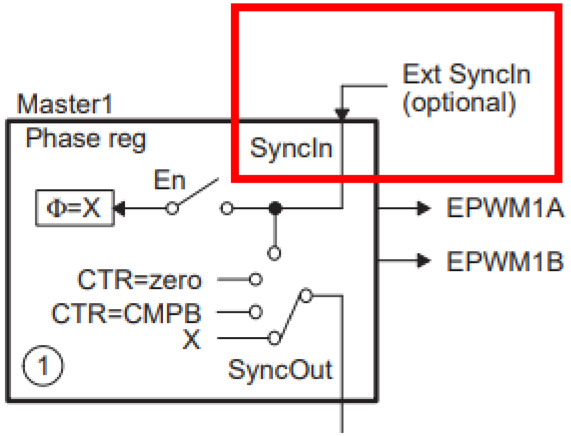

PWM module of C2000 Microcontroller

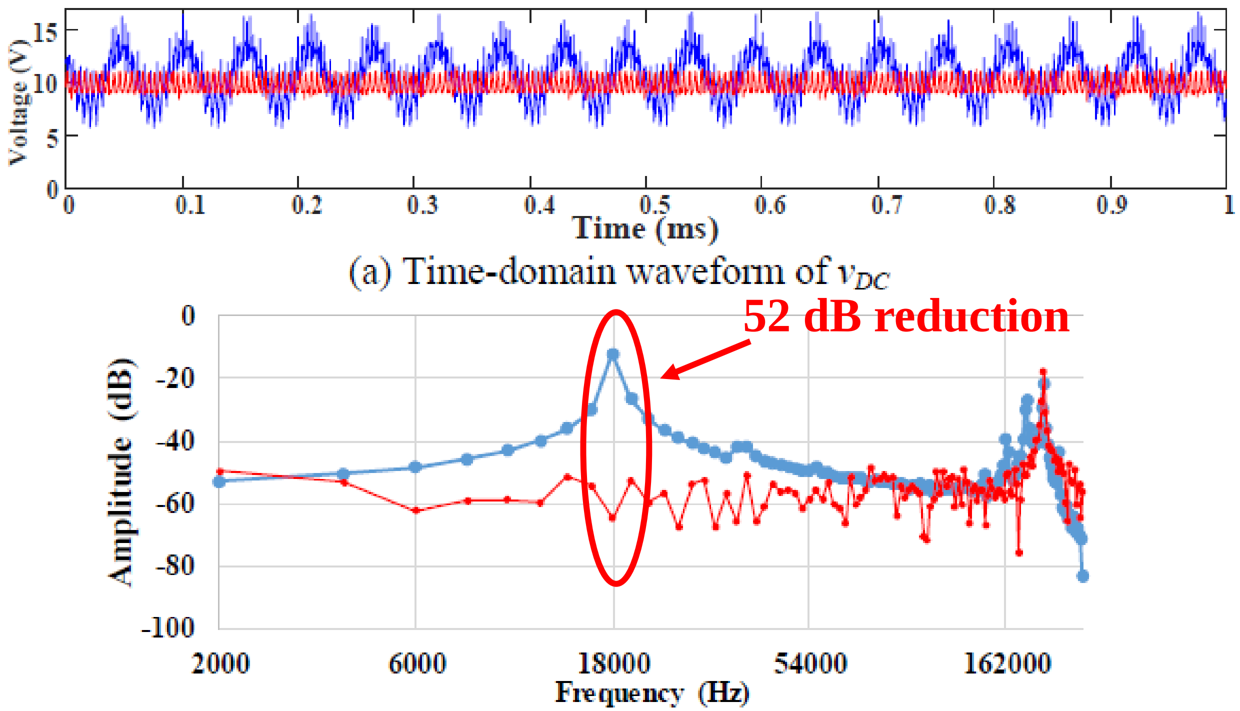

(a) Time-domain waveform of v_{DC}

(b) Normalized frequency spectrum of v_{DC}

- Frequency synchronization is the remedy

[1] **K. Li**, S. C. Tan and S. Y. R. Hui, "On Beat Frequency Oscillation of Two-Stage Wireless Power Receivers", IEEE Transactions on Power Electronics, vol. 35, no. 12, pp. 12741-12751, Dec. 2020.

Outline

- Motivation
- Challenge: Beat frequency oscillation
  - Solutions:
    - Hybrid topology
    - Modulation
- Challenge: Right-half-plane zeros
  - Solutions:
    - Control methods for alleviating the adverse effects of right-half-plane zeros
    - Control methods for eliminating the right-half-plane zeros

Hybrid topology

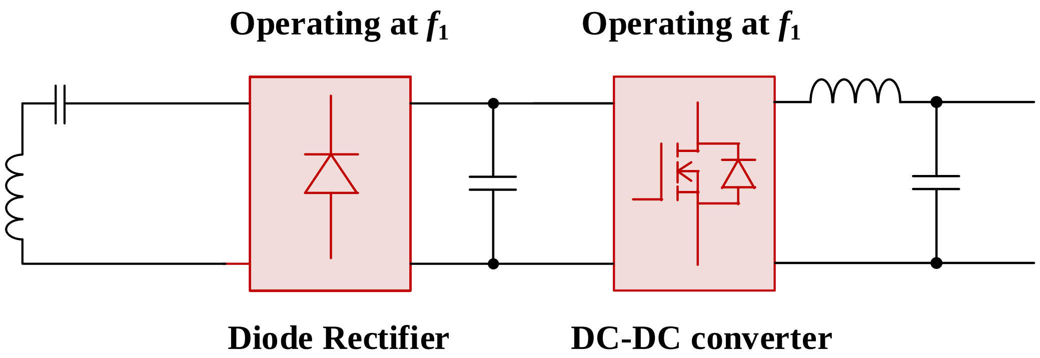

Components multiplex

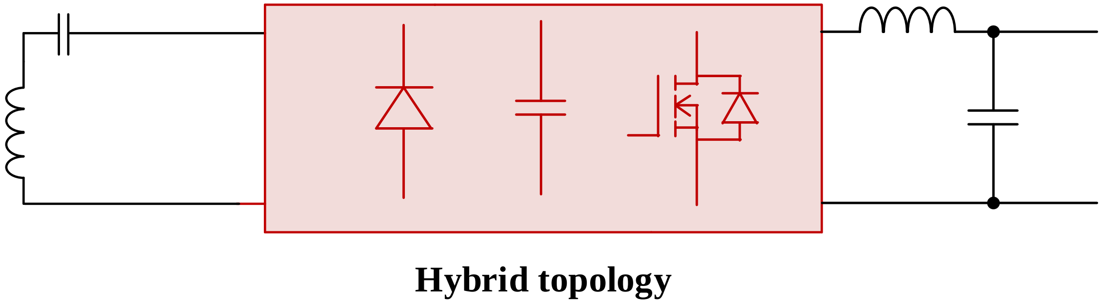

Derived topology

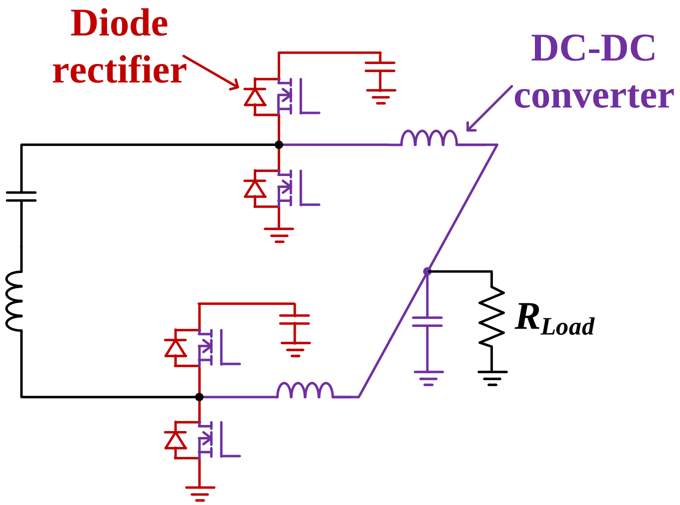

Features:
- Multiplex the MOSFETs
- Reduce component cost

Extra benefit:
- Soft switching
- Automatic current balancing
    - Extra control effort is required in DC-DC converter

[1] **K. Li**, S. C. Tan, and S. Y. R. Hui, "Efficient Hybrid-Modulated Single-Stage Wireless Power Receiver with Continuous DC Current", IEEE Transactions on Power Electronics, vol. 36, no. 12, pp. 13504-13514, Dec. 2021.
[2] **K. Li**, S. C. Tan, and S. Y. R. Hui, “Interleaved Buck-Type Rectifier with Pseudo-DC-Link Capacitors for Automatic Current Balancing”, IEEE Transactions on Industrial Electronics, Early access

Hybrid topology

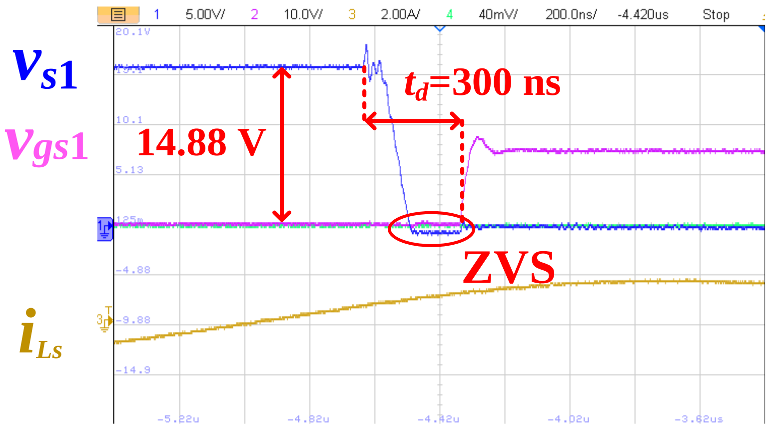

ZVS turn-on of S_1

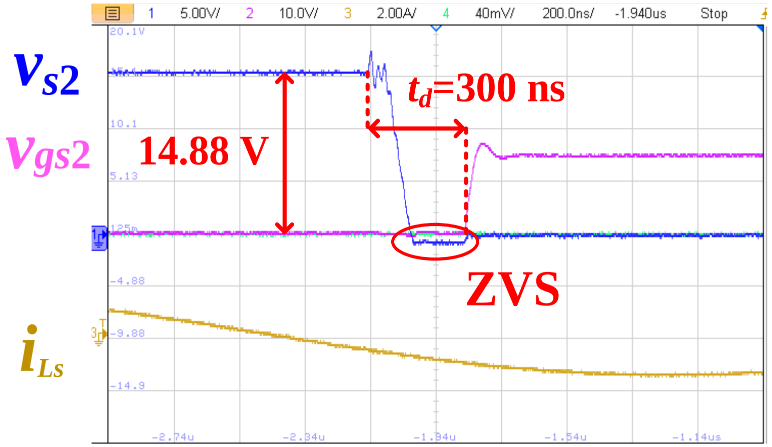

ZVS turn-on of S_2

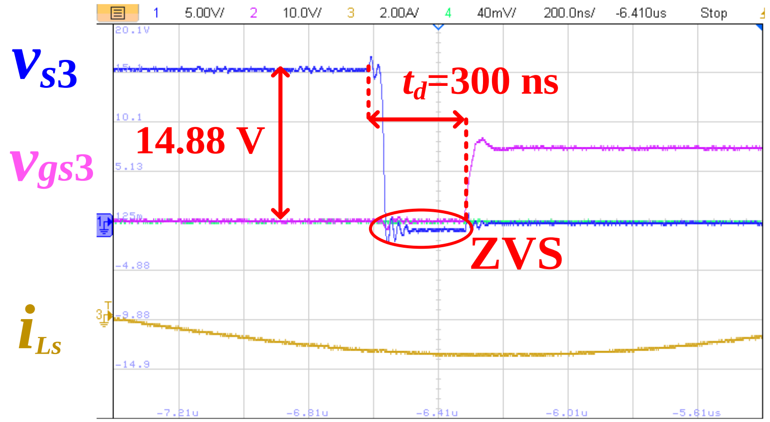

ZVS turn-on of S_3

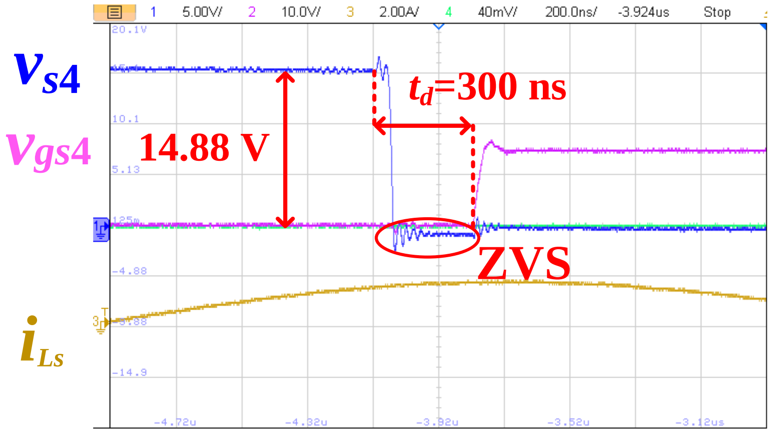

ZVS turn-on of S_4

Fully soft-switching operation for the switches

Hybrid topology

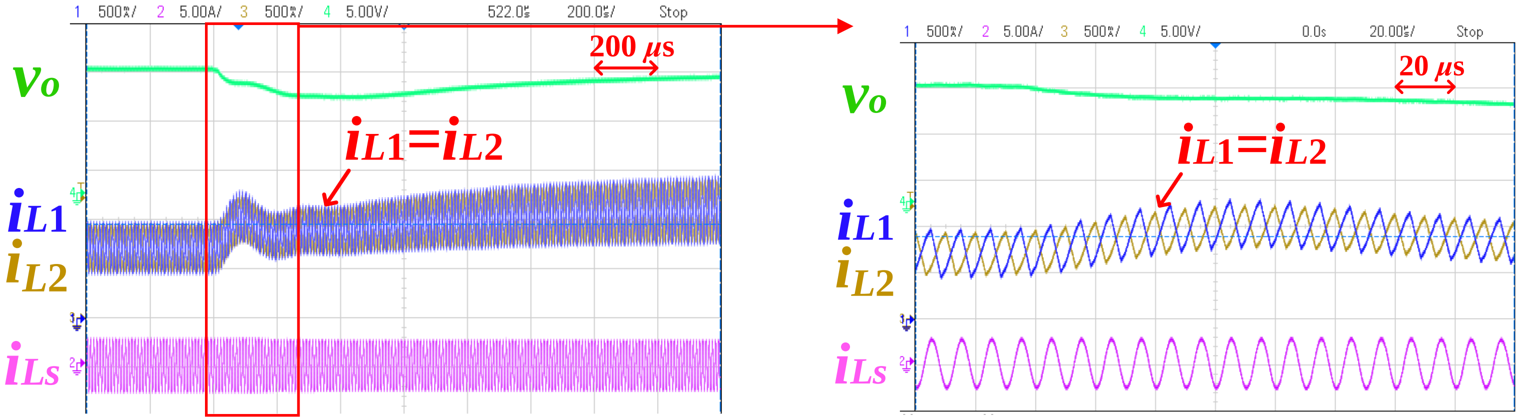

Current balancing during dynamic response

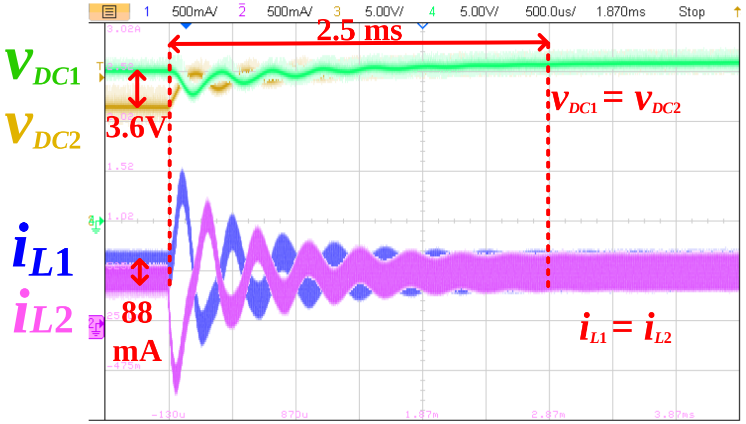

$$C_{DC}L\frac{d^2(i_{L1}-i_{L2})}{dt^2}+C_{DC}r\frac{d(i_{L1}-i_{L2})}{dt}+D^2(i_{L1}-i_{L2})=0$$

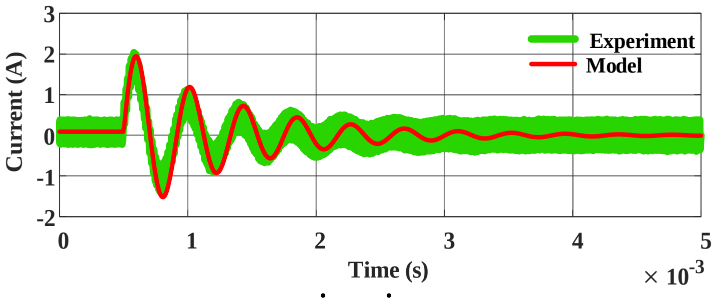

$i_{L1}-i_{L2}$

Current balancing after disturbance

Automatic current balancing

Outline

- Motivation
- Challenge: Beat frequency oscillation
  - Solutions:
    - Hybrid topology
    - Modulation
- Challenge: Right-half-plane zeros
  - Solutions:
    - Control methods for alleviating the adverse effects of right-half-plane zeros
    - Control methods for eliminating the right-half-plane zeros

Modulation

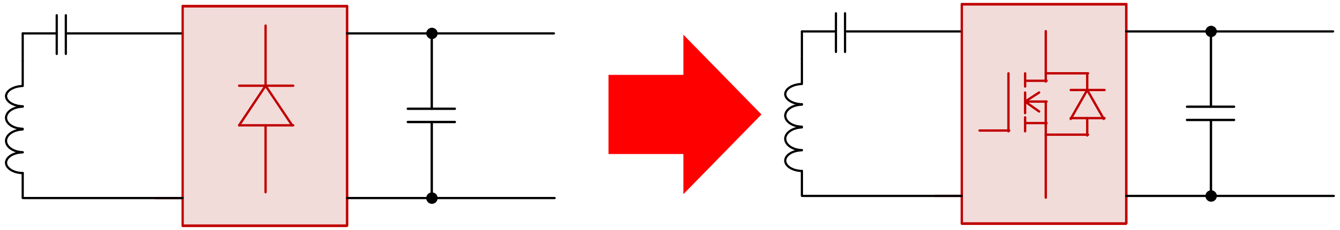

Resonant Rectifier

Use active switch

Resonant Rectifier

Derived topology

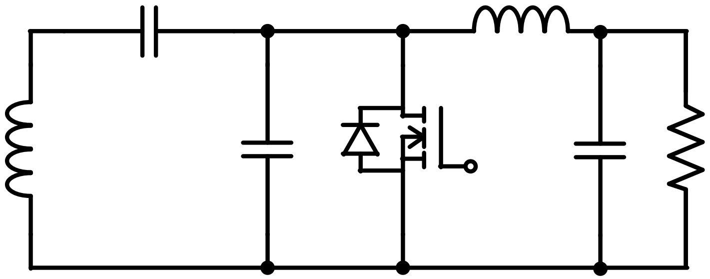

Single-phase class E rectifier

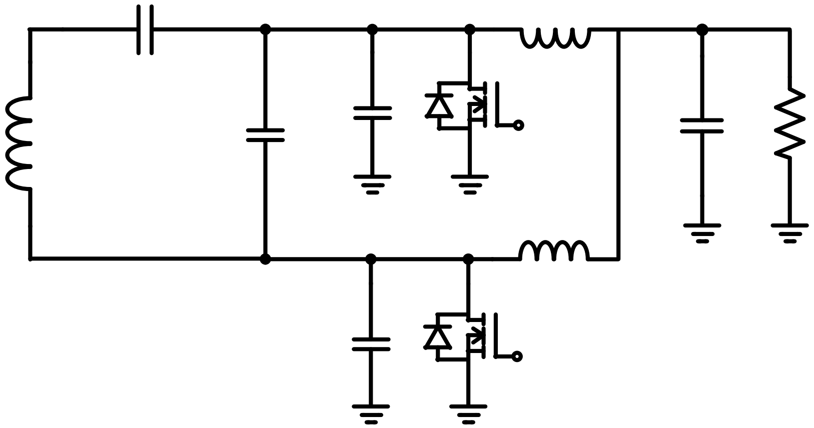

Differential class E rectifier

Features:

1. Minimize the number of semiconductors
2. Inherent soft-switching operation

Drawback:

1. Unregulated output

[1] **K. Li**, S. C. Tan and S. Y. R. Hui, "Low-Cost Single-Switch Bidirectional Wireless Power Transceiver for Peer-To-Peer Charging", IEEE Journal of Emerging and Selected Topics in Power Electronics, vol. 9, no. 3, pp. 3781-3790, June 2021.
[2] **K. Li**, S. C. Tan and S. Y. R. Hui, "Single-Stage Regulated Resonant WPT Receiver with Low Input Harmonic Distortion", IEEE Transactions on Power Electronics, vol. 35, no. 7, pp. 6820-6829, July 2020.
[3] **K. Li**, S. C. Tan and S. Y. R. Hui, "Single-Switch-Regulated Resonant WPT Receiver", IEEE Transactions on Power Electronics, vol. 34, no. 11, pp. 10386-10391, Nov. 2019.

Modulation

- Frequency modulation?
  - No, frequency is fixed by the wireless power transmitter.

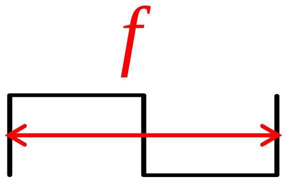

- Pulse-width modulation?
  - No, lose ZVS and lower efficiency.

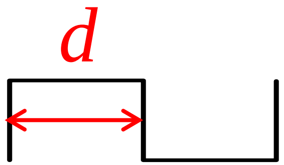

- Phase-shift modulation?
  - Maybe, but too sensitive to the phase changes

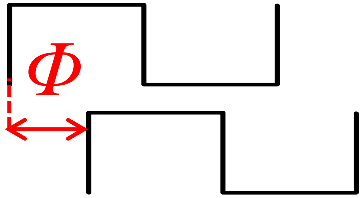

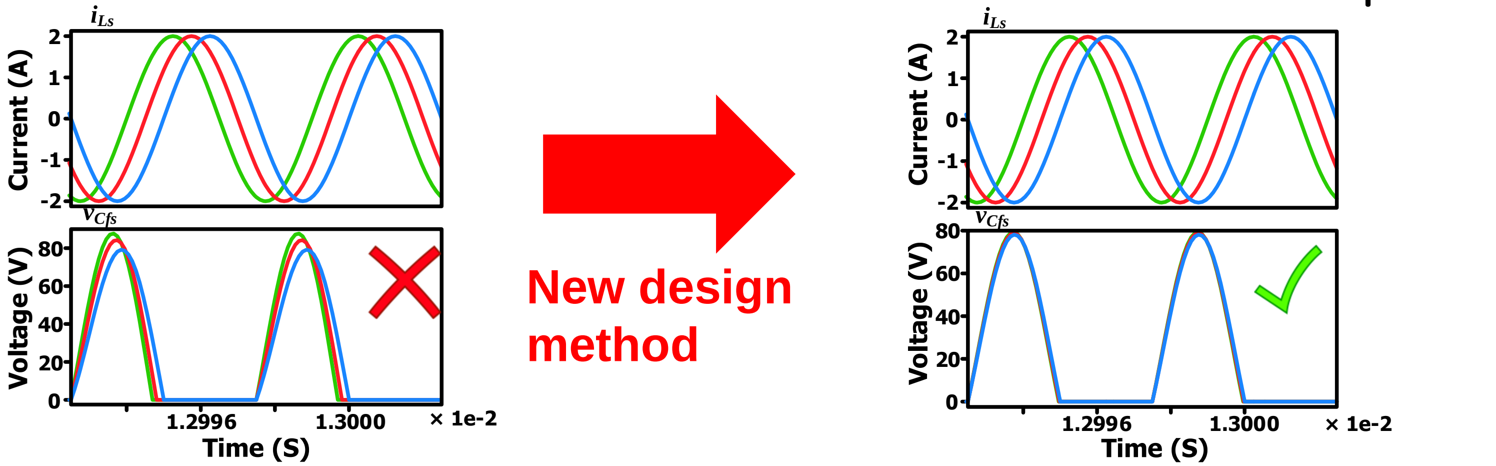

Modulation

Phase-shift based power flow control

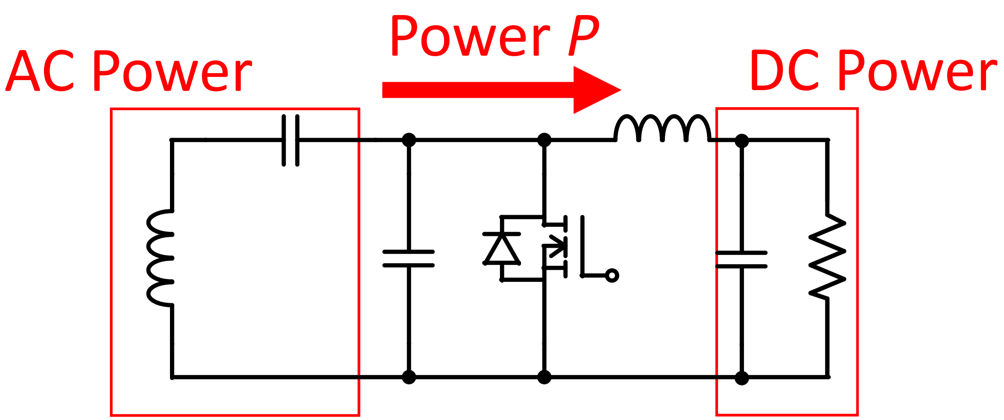

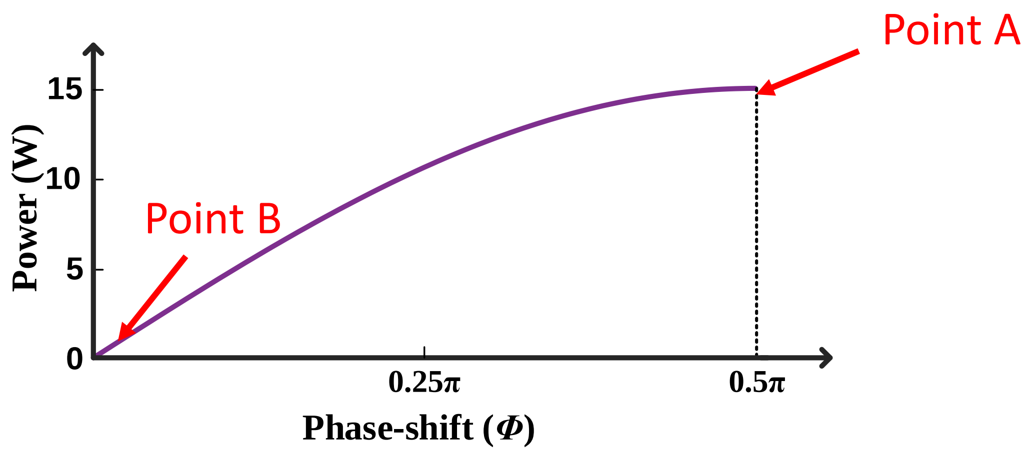

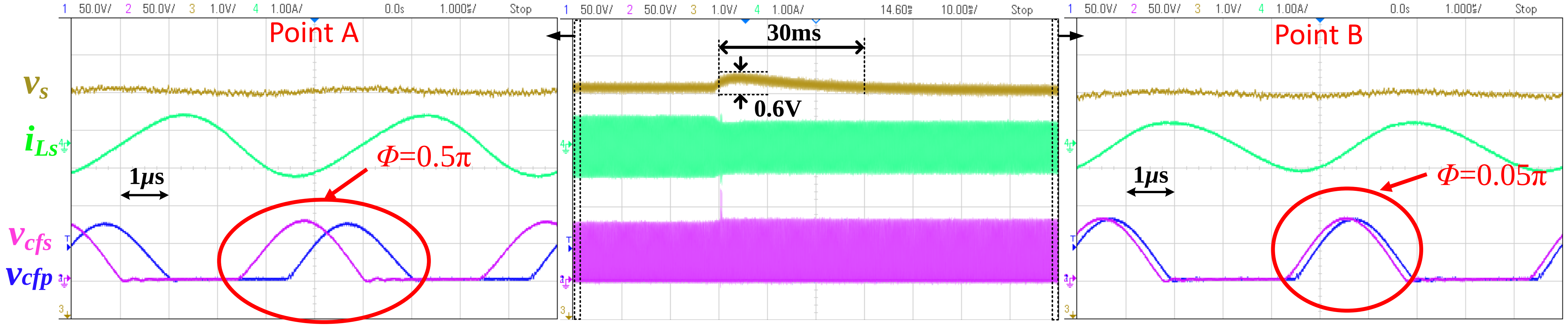

Dynamic response of power steps from 15 W to 2 W,

Modulation

Peer-to-peer charging

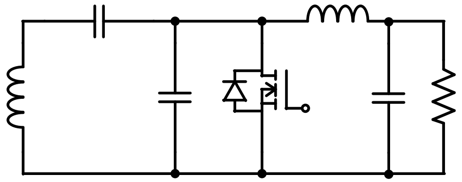

Single-stage class E rectifier

Bidirectional operation

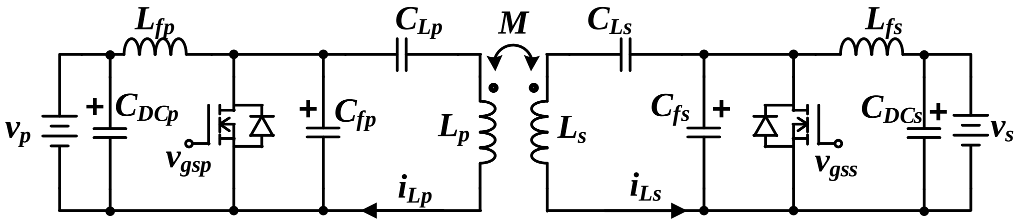

Bidirectional wireless power transfer system

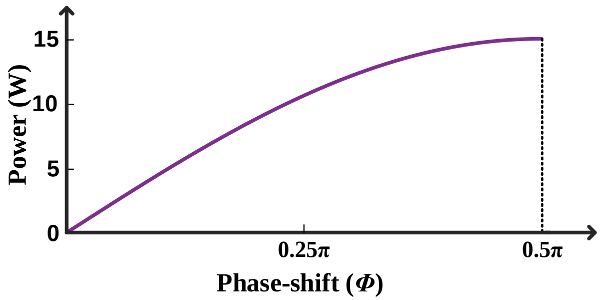

Extend phase-shift range

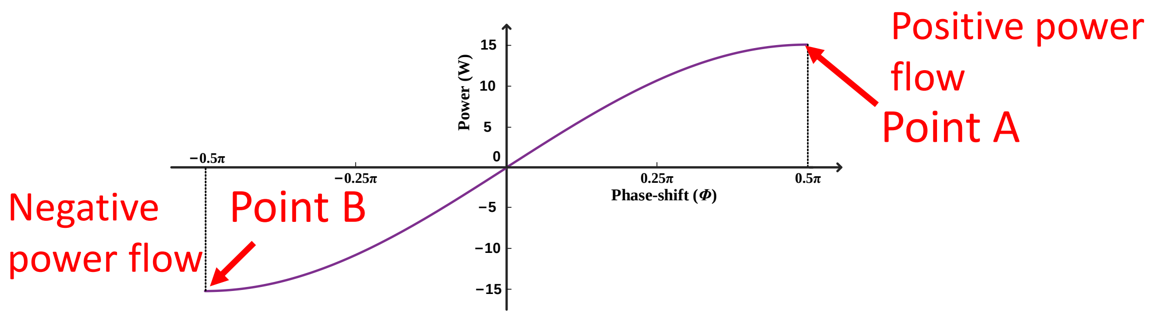

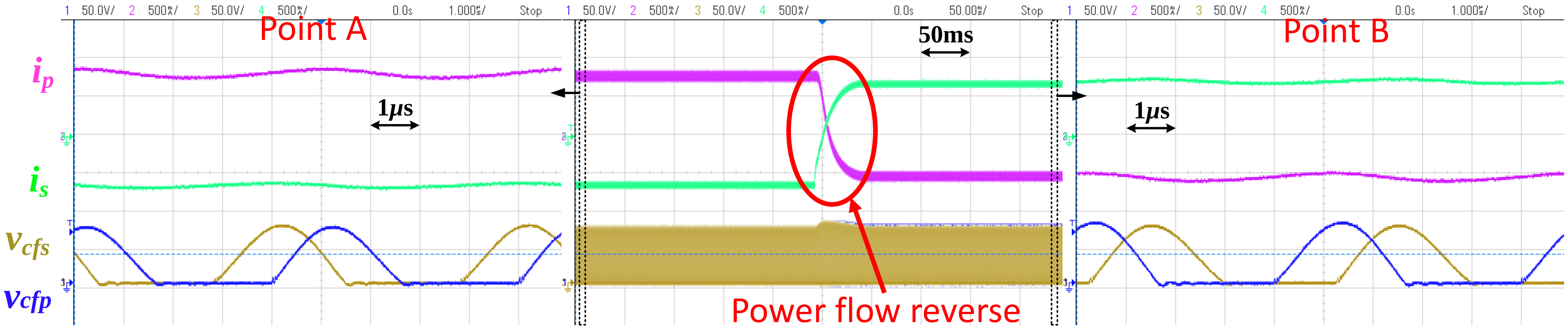

Outline

- Motivation
- Challenge: Beat frequency oscillation
    - Solutions:
        - Hybrid topology
        - Modulation
- Challenge: Right-half-plane zeros
    - Solutions:
        - Control methods for alleviating the adverse effects of right-half-plane zeros
        - Control methods for eliminating the right-half-plane zeros

Challenges

Low stability margin of DC-DC converter

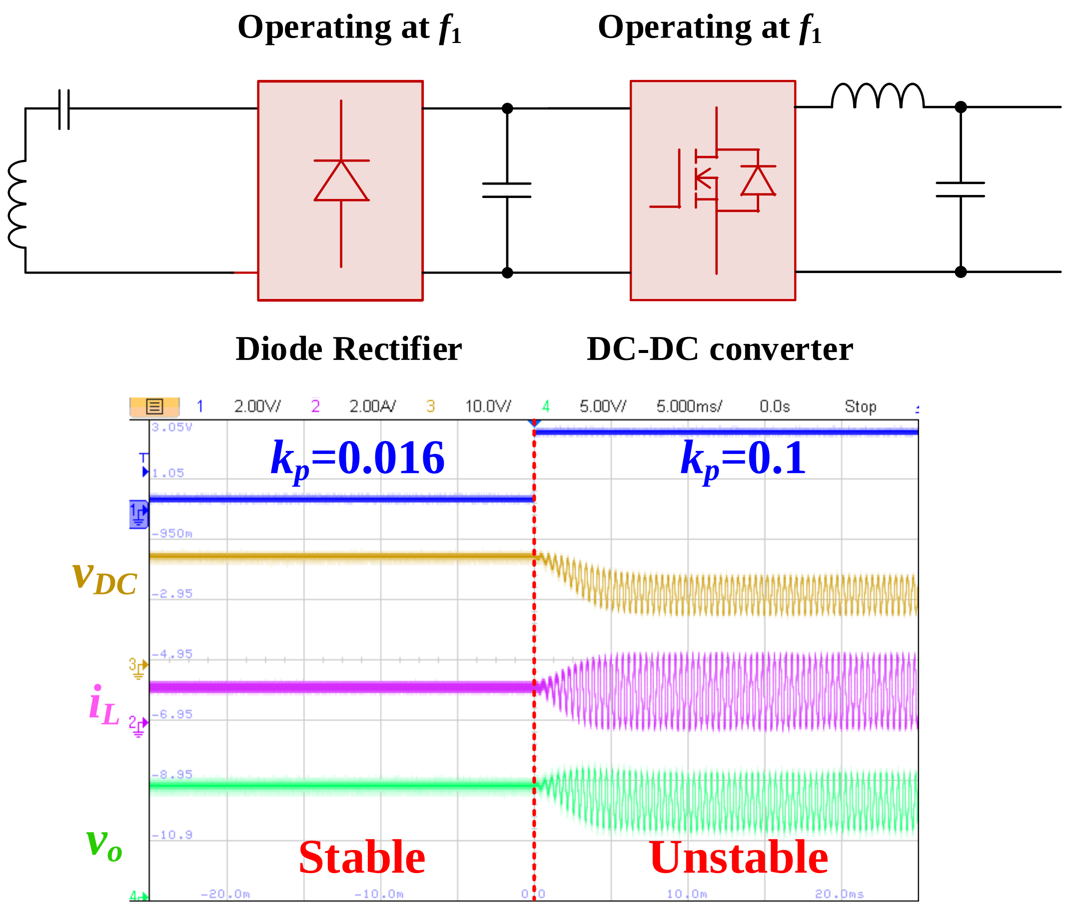

Buck converter in wireless power receiver system

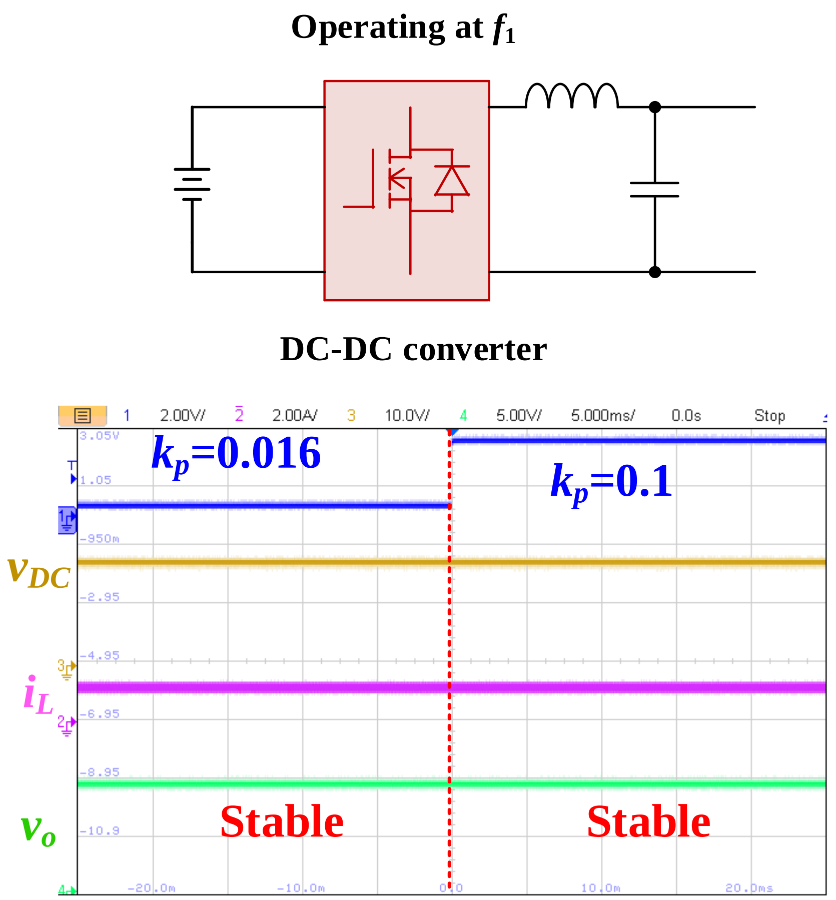

Buck converter

[1] **K. Li,** S. C. Tan and S. Y. R. Hui, "On Effect of Right-Half-Plane Zero Present in Buck Converters with Input Current Source in Wireless Power Receiver Systems", IEEE Transactions on Power Electronics, vol. 36, no. 6, pp. 6364-6374, June 2021.

Challenges

Right-half-plane zero

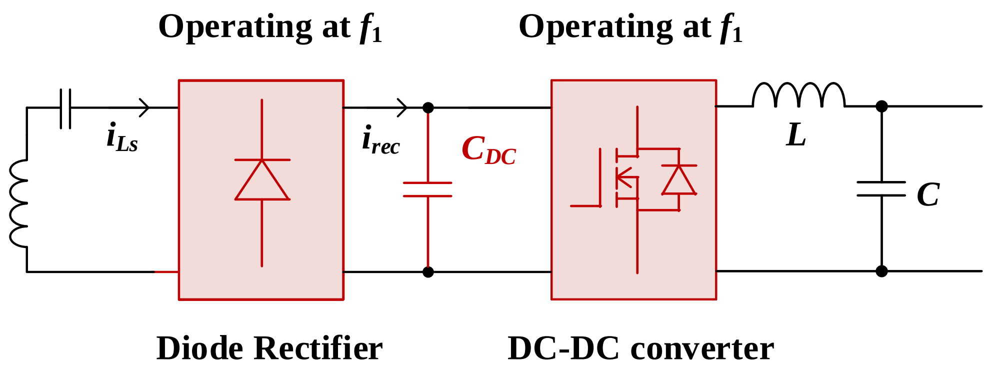

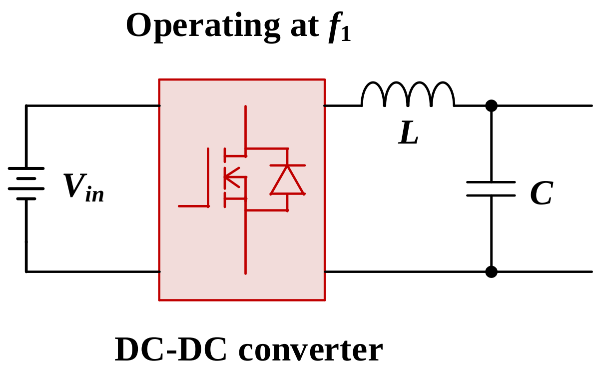

$$G_{v_o}(s) = \frac{\widetilde{v_o}}{\tilde{d}} = \frac{2RI_{Ls}(C_{DC}Rs - D^2)}{\pi D^2[C_oC_{DC}LRs^3 + C_{DC}Ls^2 + (C_oRD^2 + C_{DC}R)s + D^2]}$$

$$G(s) = \frac{\widetilde{v_o}\,(s)}{\tilde{d}\,(s)} = \frac{V_{in}}{s^2LC + s\frac{L}{R} + 1}$$

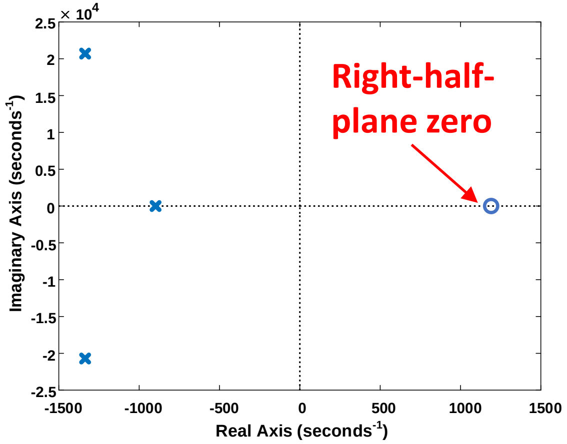

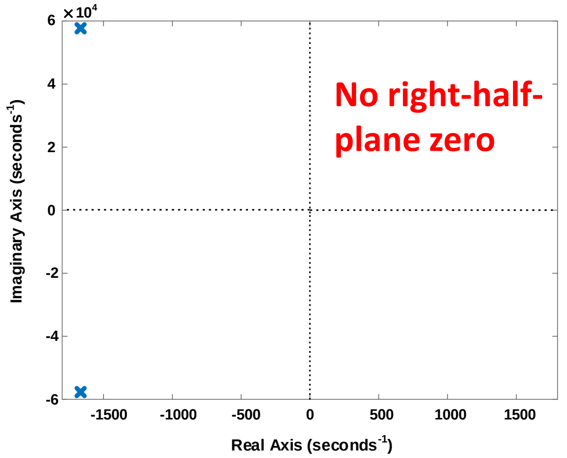

Challenges

Adverse effects: non-monotonic dynamic response

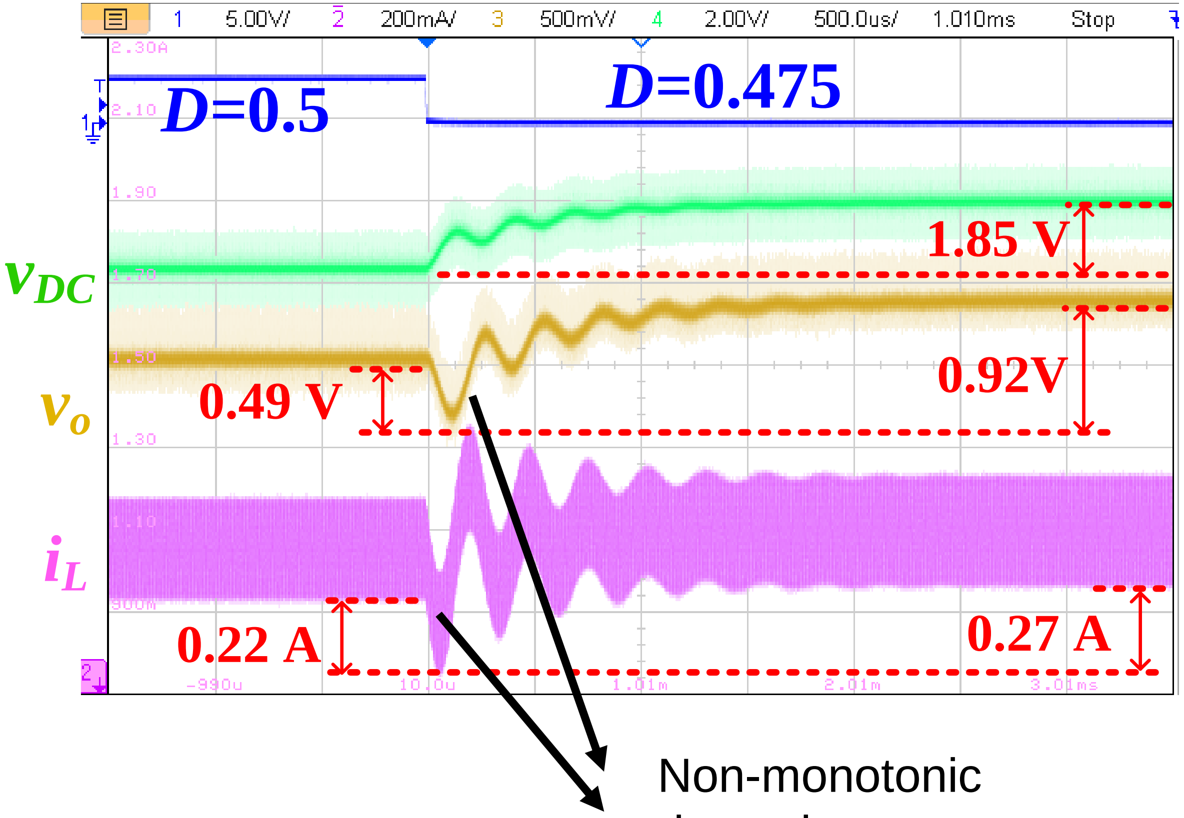

Non-monotonic dynamic response

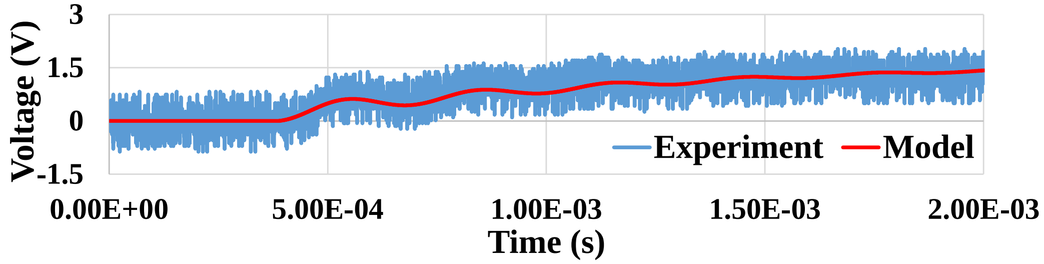

Step responses of v_{DC}

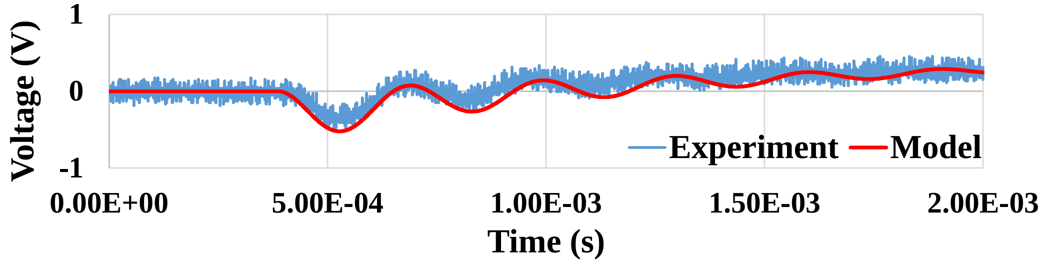

Step responses of v_o

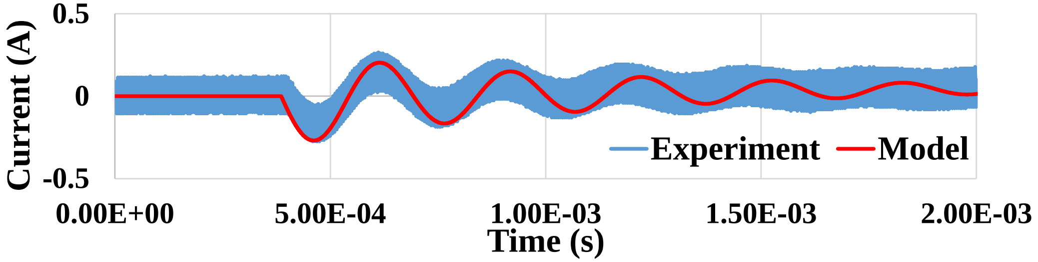

Step responses of i_L

Challenges

Adverse effects: Transmitter-side current overshoot

Simulation results

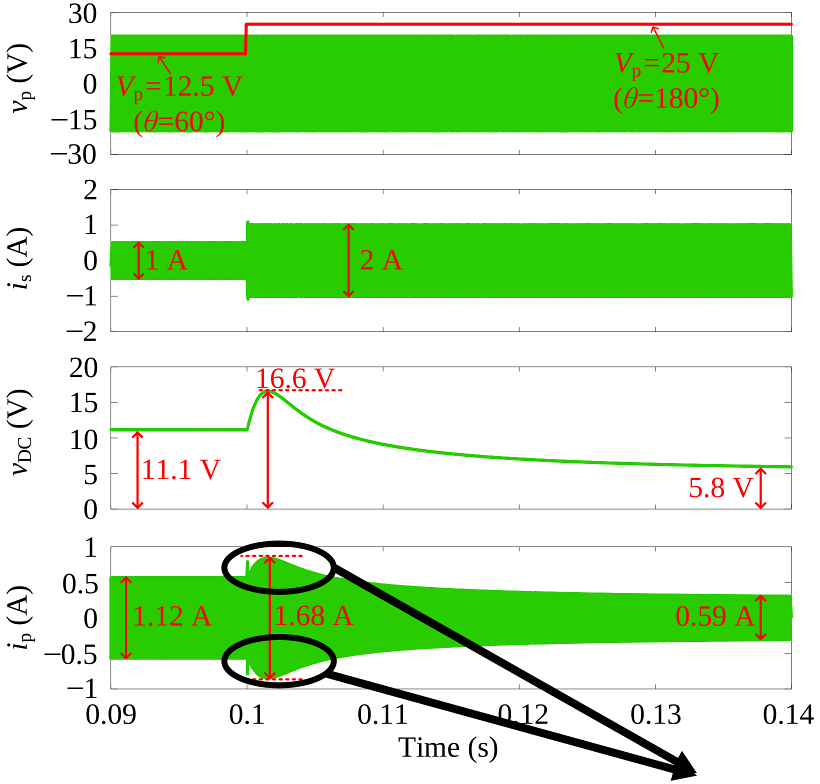

Experimental results

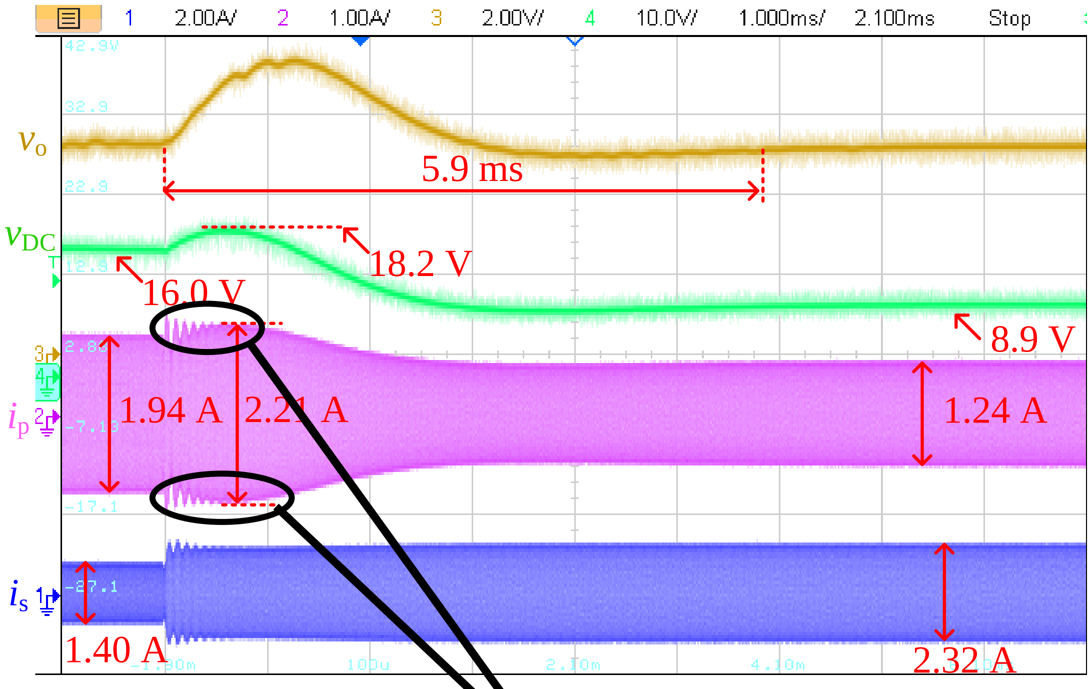

Current overshoot

Current overshoot

Outline

- Motivation
- Challenge: Beat frequency oscillation
  - Solutions:
    - Hybrid topology
    - Modulation
- Challenge: Right-half-plane zeros
  - Solutions:
    - Control methods for alleviating the adverse effects of right-half-plane zeros
    - Control methods for eliminating the right-half-plane zeros

Control

DC-link voltage feedforward

Increase the frequency of the right-half-plane zero

$$s = \frac{D^2}{C_{DC}R}$$

Introduce a virtual damping resistor R_{damp} to reduce R

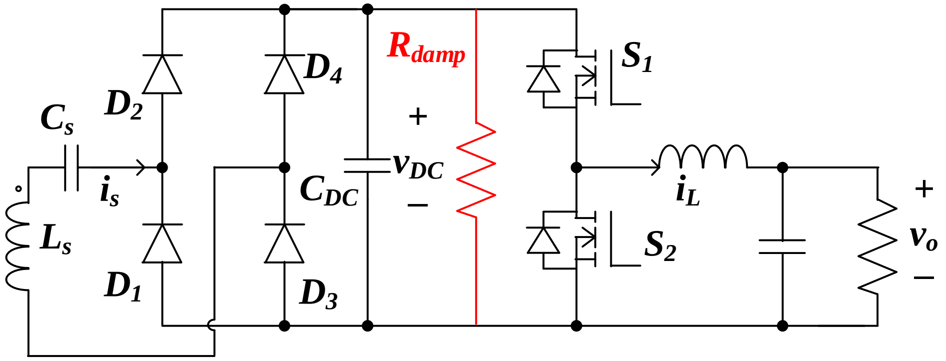

Path A is equivalent to a physical damping resistor (R_{damp}=1/k_{damp})

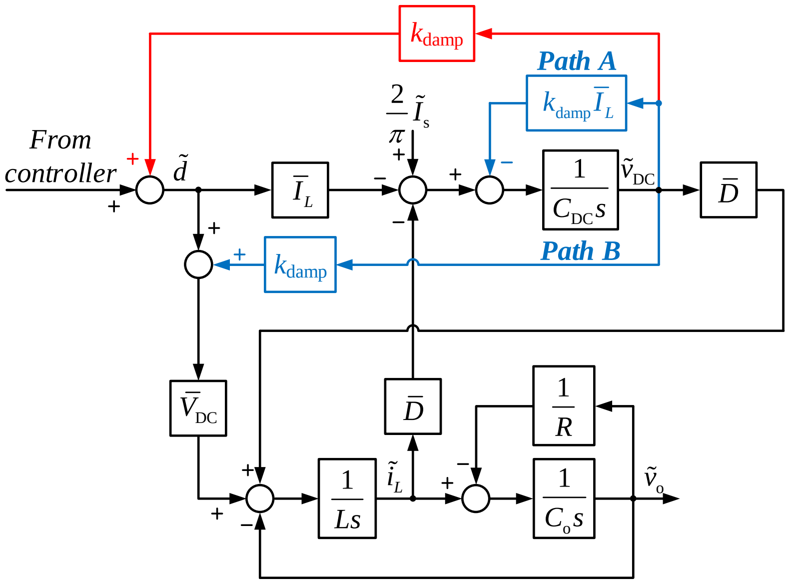

DC-link voltage feedforward

[1] **K. Li**, H. Yuan, S. C. Tan, and S. Y. R. Hui, "Overshoot Damping and Dynamics Improvement in Wireless Power Transfer Systems via Receiver-Side Controller Design", *IEEE Transactions on Power Electronics*, vol. 37, no. 2, pp. 2362-2371, Feb. 2022.

Control

DC-link voltage feedforward

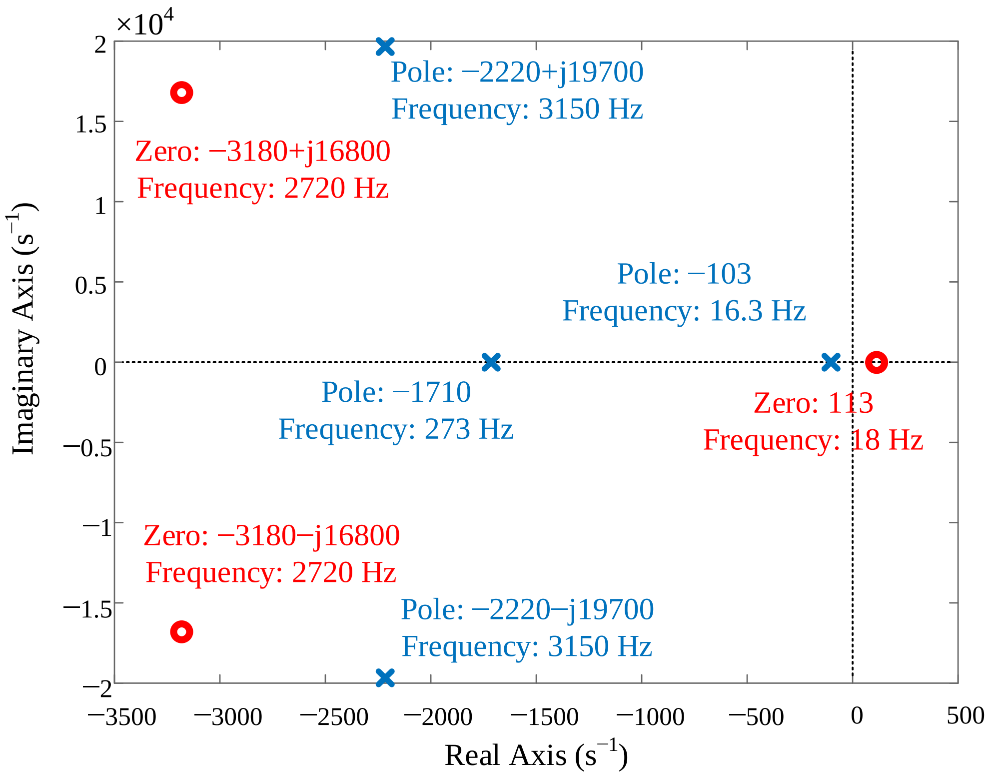

Without feedforward

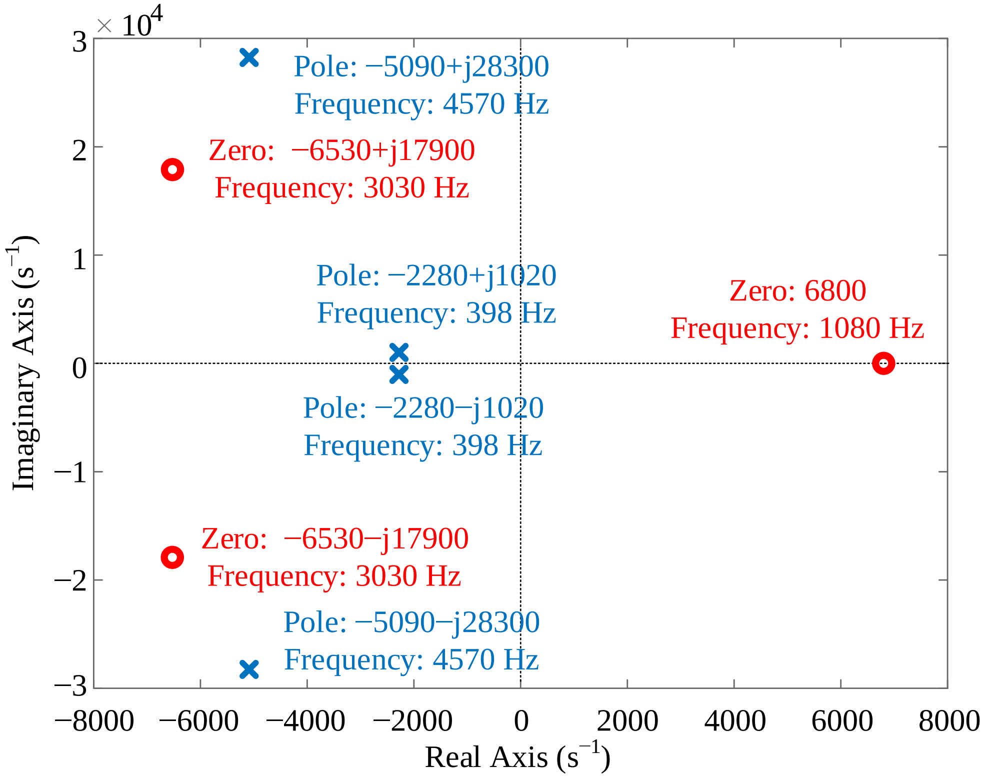

With feedforward

The right-half-plane zero can be significantly increased (from 18 Hz to 1080 Hz)

Control

DC-link voltage feedforward

i_s step change

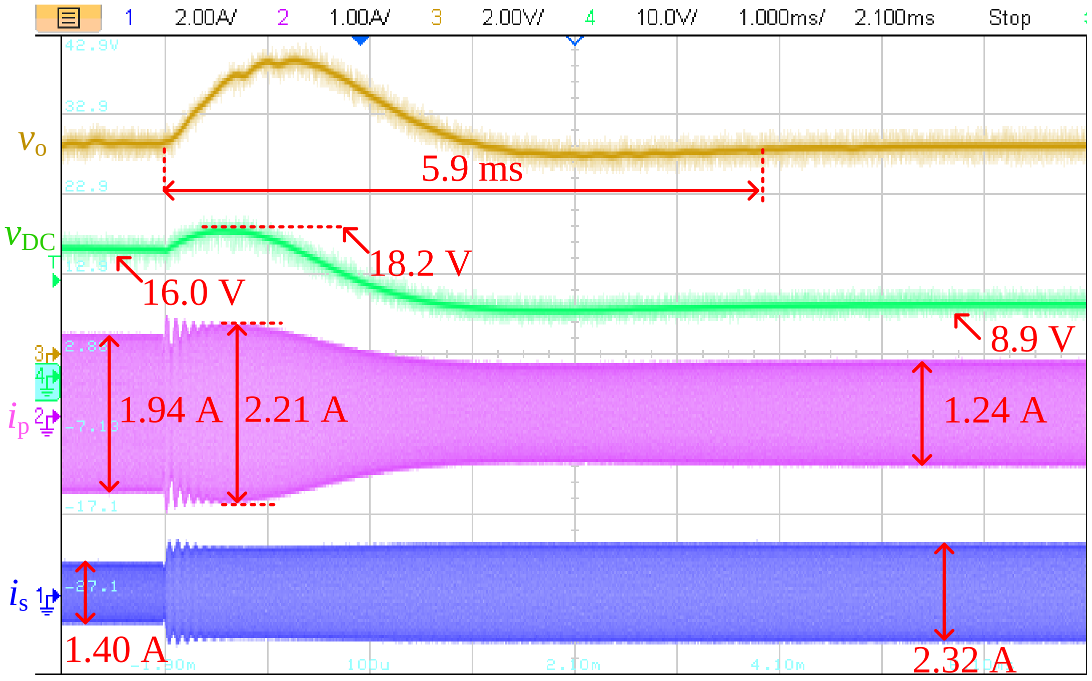

Without feedforward

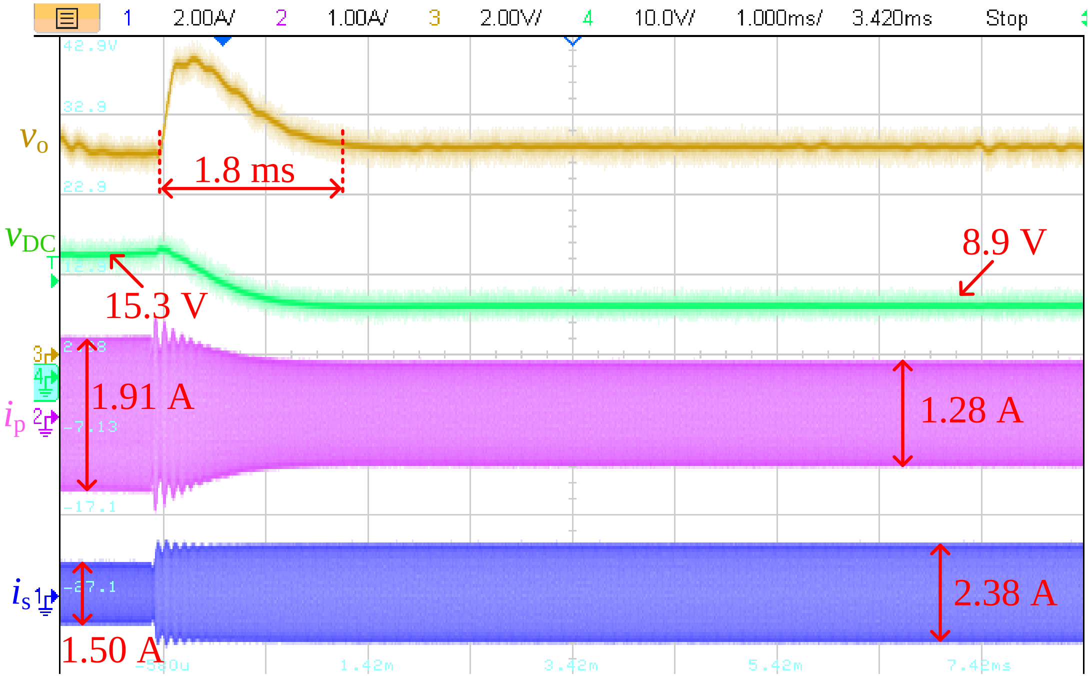

With feedforward

The overshoot is alleviated

The dynamic response is improved

Control

DC-link voltage feedforward

i_o step change

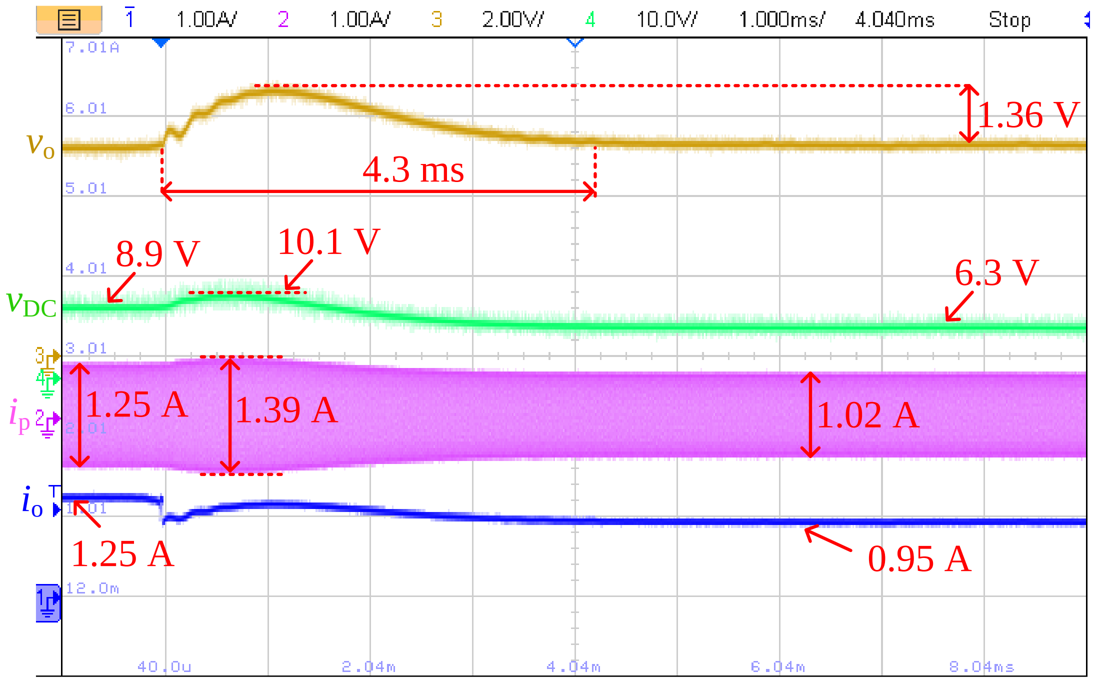

Without feedforward

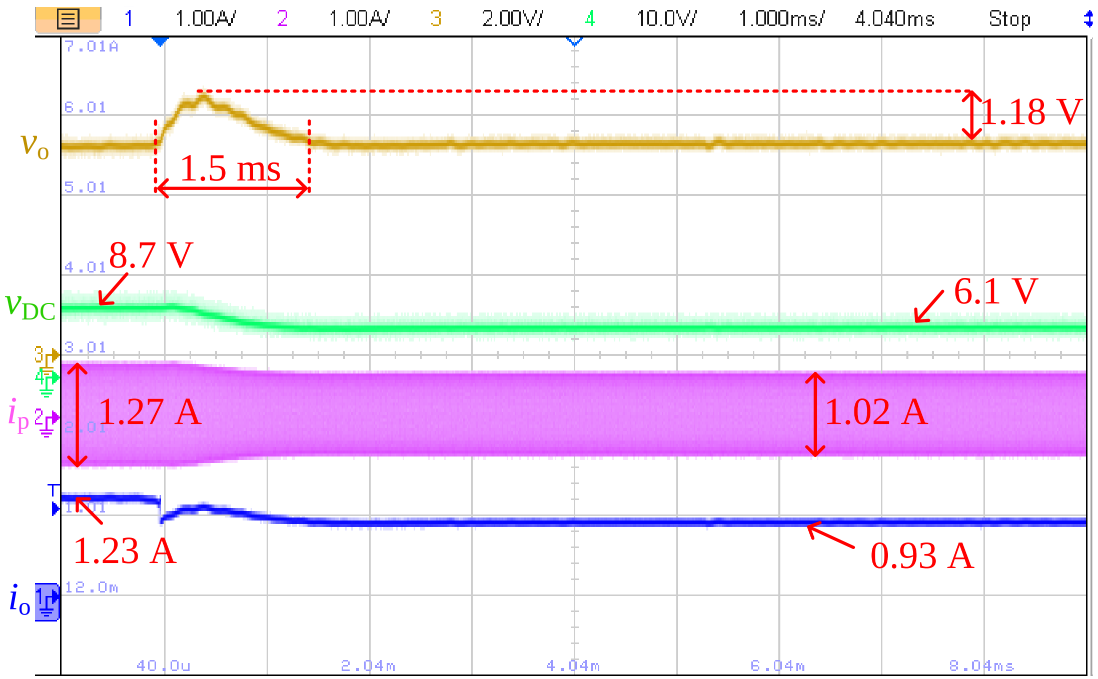

With feedforward

The dynamic response is also improved

Outline

- Motivation
- Challenge: Beat frequency oscillation
  - Solutions:
    - Hybrid topology
    - Modulation
- Challenge: Right-half-plane zeros
  - Solutions:
    - Control methods for alleviating the adverse effects of right-half-plane zeros
    - Control methods for eliminating the right-half-plane zeros

Control

Elimination of the right-half-plane zero

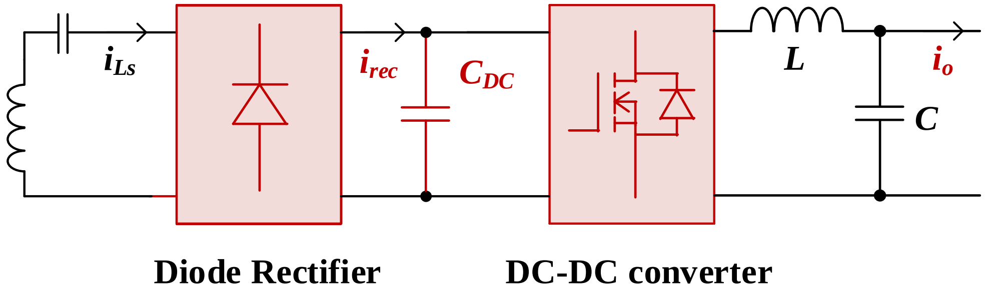

Introduce active switches

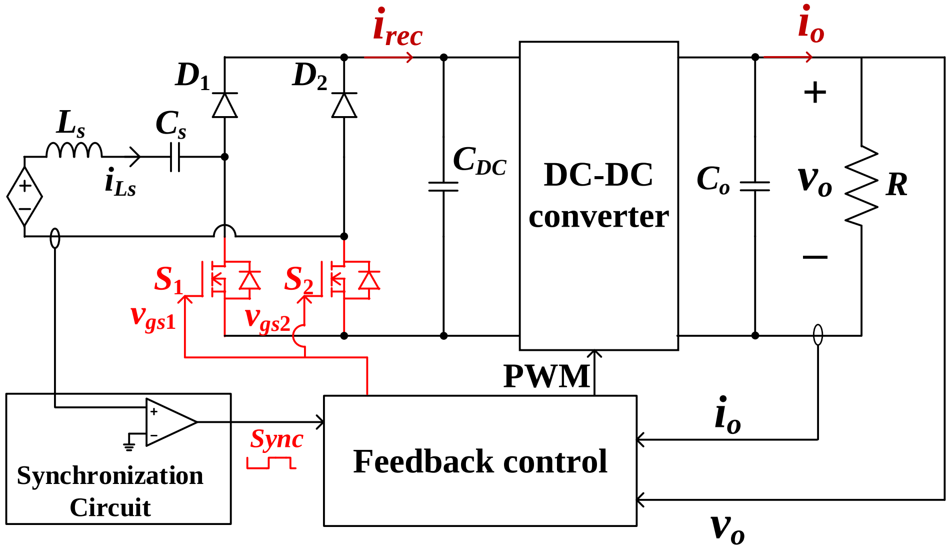

- i_{rec} is source dependent (uncontrollable)
- i_o is load dependent (unregulated)
- Temporary current imbalance leads to the right-half-plane zero

- i_{rec} can be controlled by the active switches
- i_o can be regulated by the feedback control
- Current imbalance is compensated and the right-half-plane zero is eliminated

[1] **K. Li**, S. C. Tan, and S. Y. R. Hui, "Dynamic Response and Stability Margin Improvement of Wireless Power Receiver Systems via Right-Half-Plane Zero Elimination", *IEEE Transactions on Power Electronics*, vol. 36, no. 10, pp. 11196-11207, Oct. 2021.

Control

Elimination of the right-half-plane zero

Original one (with diode rectifier)

$$G_{buck}(s) = \frac{2RI_{Ls}(C_{DC}Rs - D_{DC-DC}^2)}{\pi D_{DC-DC}^2 [C_o C_{DC} LRs^3 + C_{DC}Ls^2 + (C_o R D_{DC-DC}^2 + C_{DC}R)s + D_{DC-DC}^2]}$$

Modified one (with active rectifier)

$$G_{M_{buck}}(s) = \frac{2D_{DC-DC}I_{Ls}R\sin(2\pi D)}{[C_o C_{DC} LRs^3 + C_{DC}Ls^2 + (C_o R D_{DC-DC}^2 + C_{DC}R)s + D_{DC-DC}^2]}$$

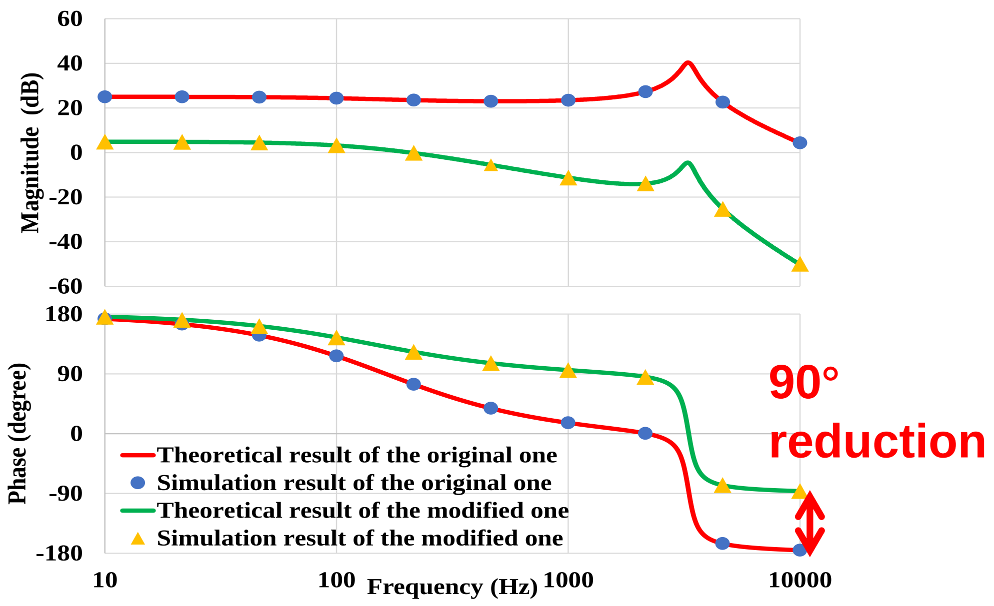

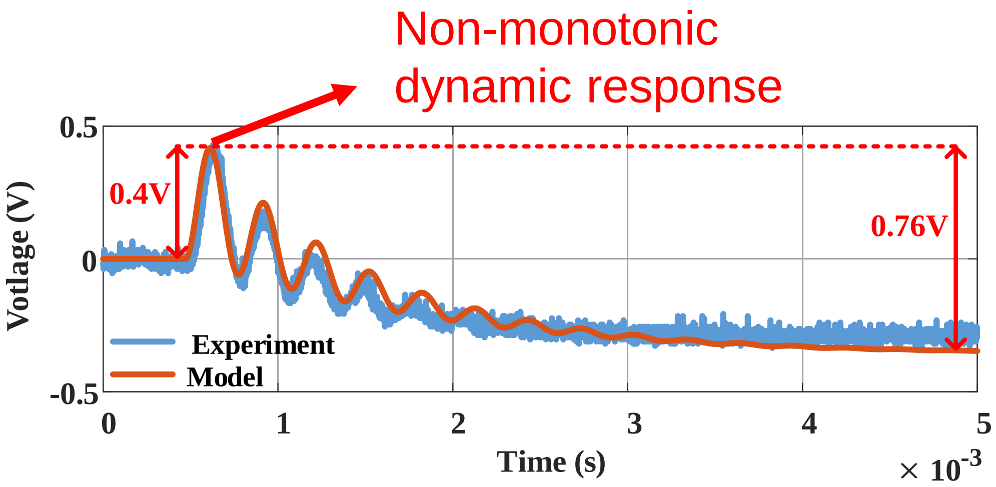

Original one (with diode rectifier)

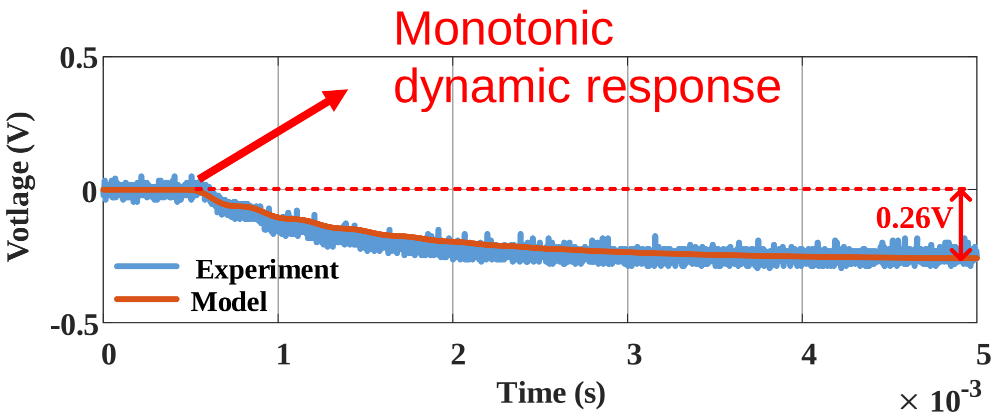

Modified one (with active rectifier)

Control

Elimination of the right-half-plane zero

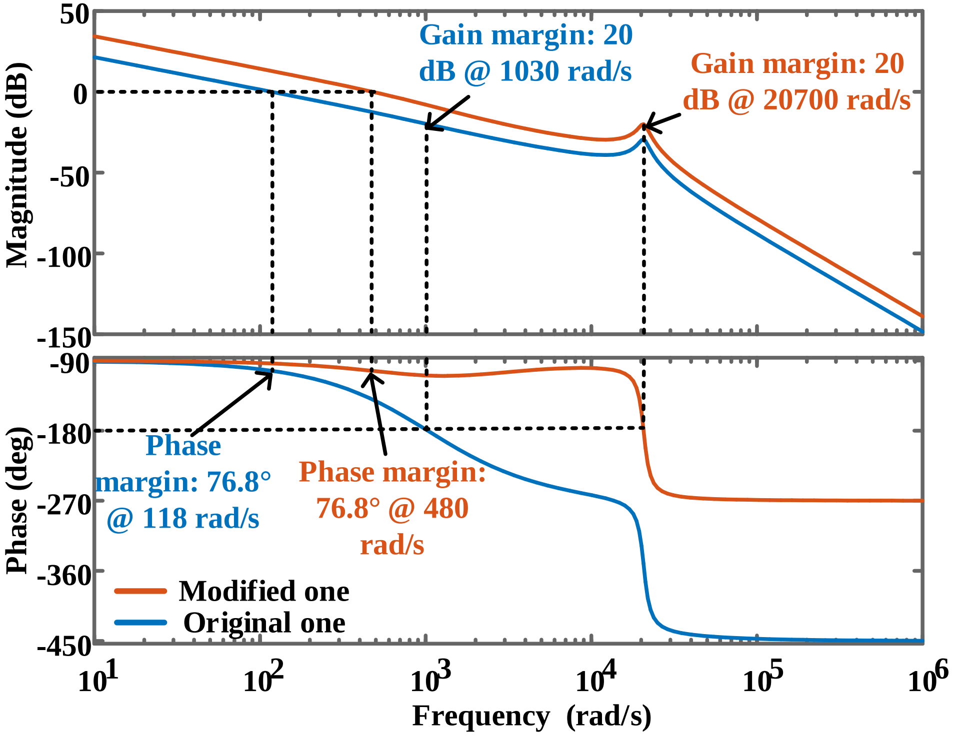

Both system has identical stability margin (Gain margin 20 dB & Phase margin 76.8°)

Dynamic response is improved

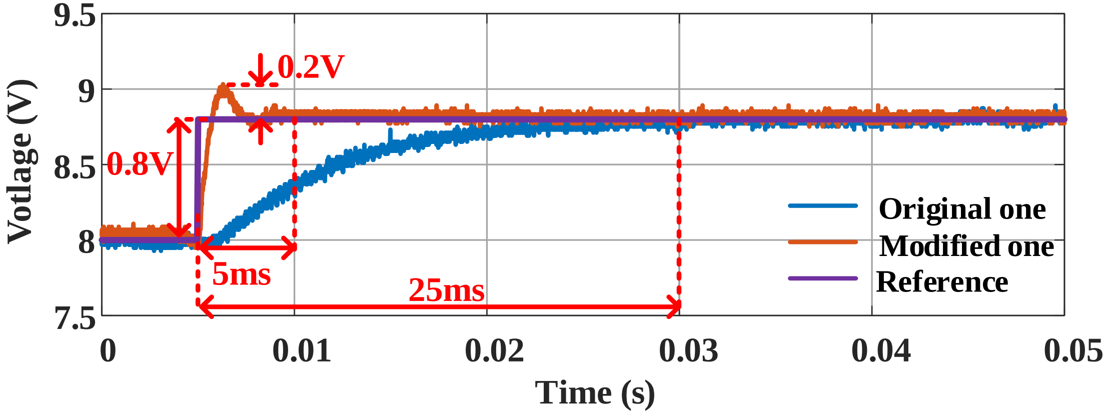

Dynamic responses of the step change of the reference voltage

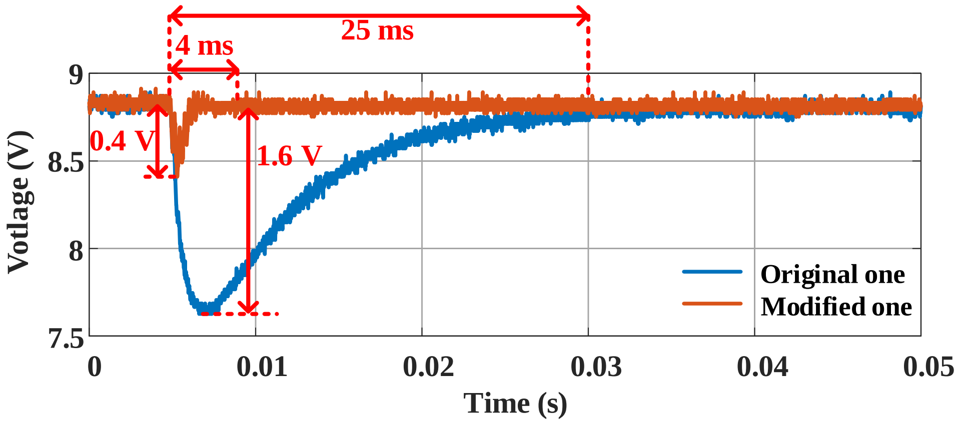

Dynamic responses of load disturbances under output voltage regulation

Control

Elimination of the right-half-plane zero

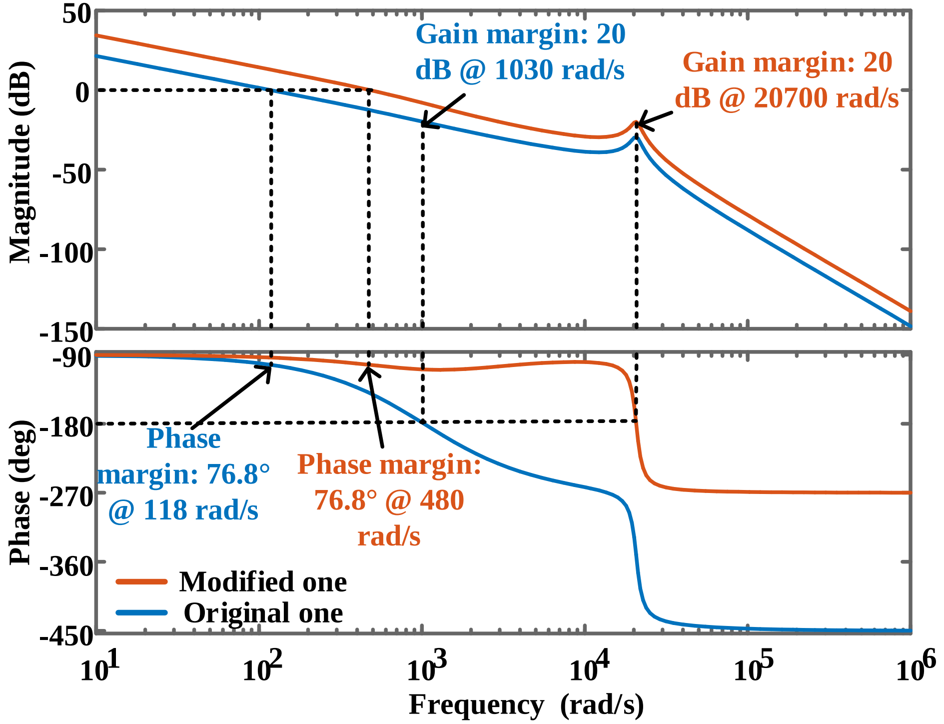

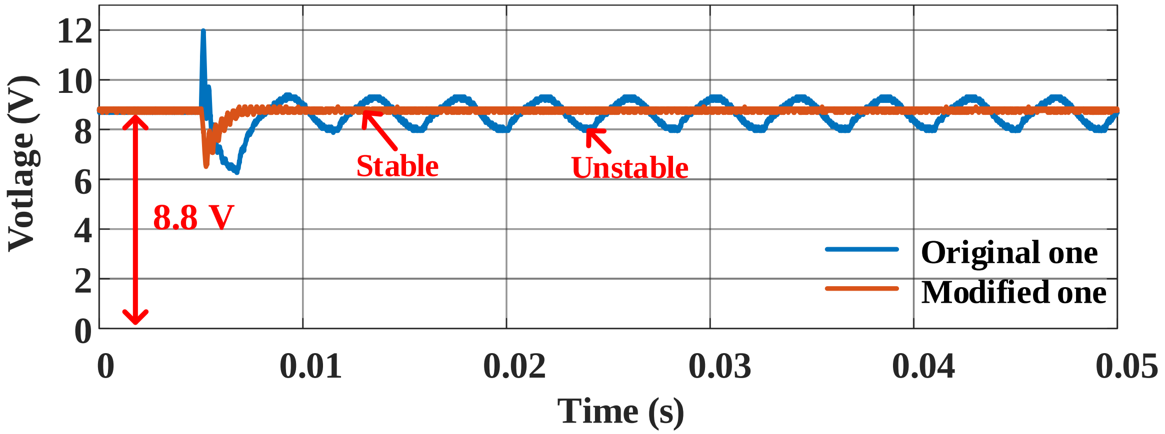

Increase the unity-gain bandwidth to 1030 rad/s

- The original system become unstable
- The modified system remains stable

Stability margin is improved

Conclusions

- Identify two new challenges
  - Beat frequency oscillations
  - Right-half-plane zeros
- Hybrid topologies
  - Multiplex the semiconductors
  - Enable soft switching operation
  - Automatic load current sharing
- Phase-shift modulation for resonant rectifiers
  - Single-stage output regulation
  - Bidirectional power flow control (peer-to-peer charging)
- New control methods are developed
  - Emulate a virtual resistance to alleviate the adverse effects of right-half-plane zeros
  - Compensate the current imbalance and eliminate the right-half-plane zeros

Part B: Multi-Coil Mid-Range Wireless Power Transmission Systems

Outline

- Motivation
- Challenge: Mid-range WPT for power grid monitoring equipment
  - Solution:
    - Planar PCB resonant winding
    - Multi-coil WPT system over insulation distance
- Challenge: Dynamic Modelling, load identification and Control
  - Solutions:
    - Dynamic Modeling Using Phasor Transformation
    - Dynamic Load Identification and Control

Mid-range Wireless power transfer

- Two-coil WPT system
  - Efficiency drops quickly over long distance
  - Diameter of windings need to be large

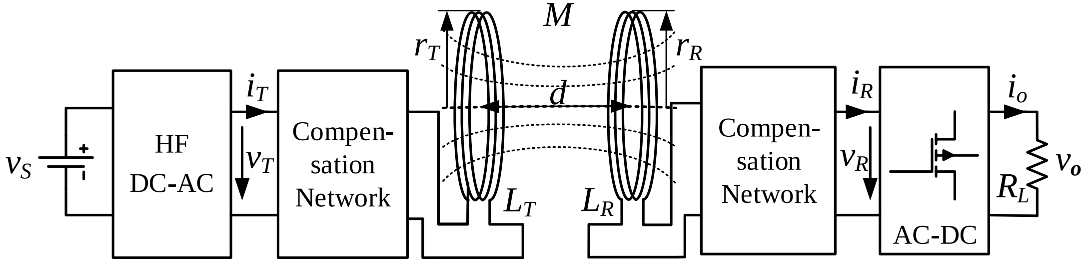

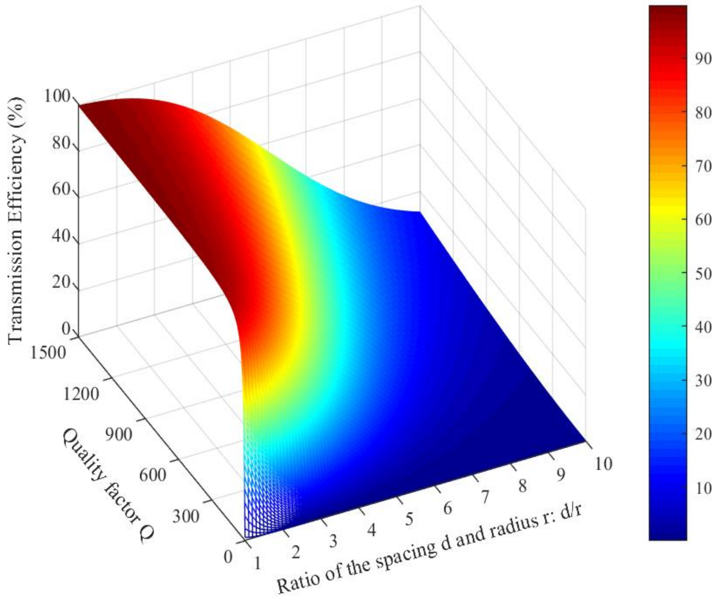

- Multi-coil WPT system

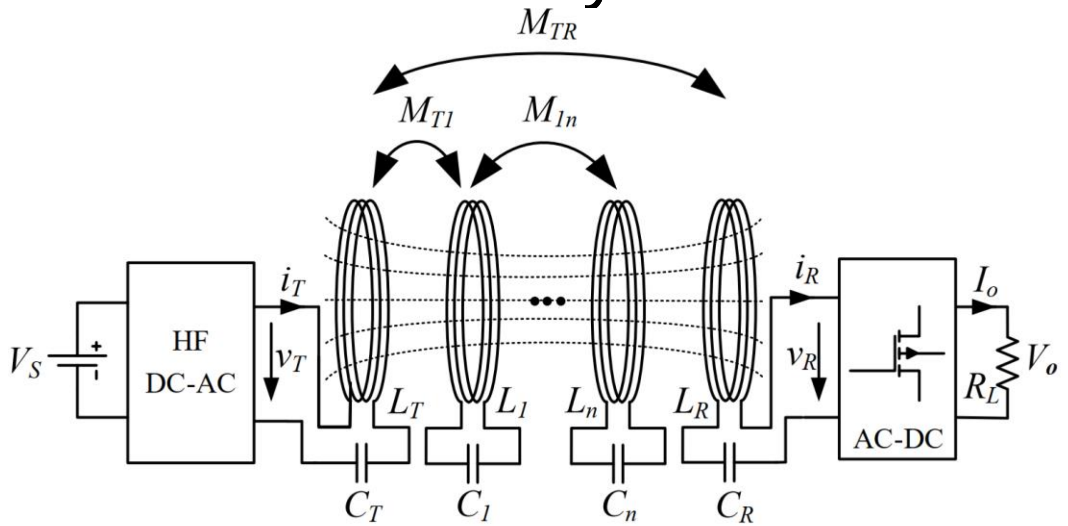

- Relay coils are placed to prevent the magnetic field from weakening
- Reasonable efficiency over insulation distance

Application

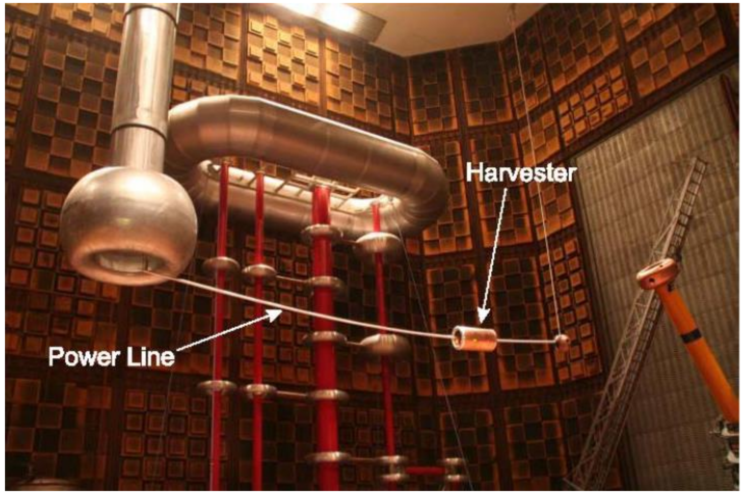

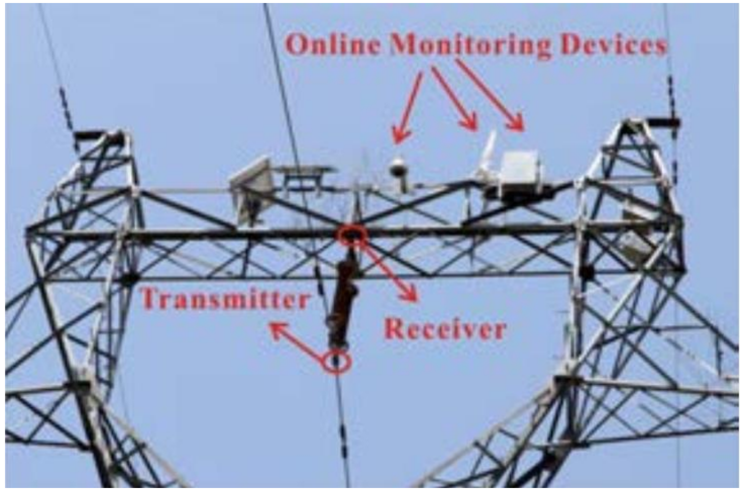

Solar Power or Wind Power

- Can work independently with power line ✓
- Subject to geographical and weather ✘
- Require large energy storing device ✘

Electric Field

- Easy to attach to power line ✓
- Performance limited by size and weight ✘
- Power rate is low (hundreds of mW) ✘

Magnetic Field – Mid-range WPT

- Stable and reliable power source ✓
- Maintain efficiency over insulation distance ✓
- Windings and capacitor to be integrated ?
- Need to pass high voltage test ?

Outline

- Motivation
- Challenge: Mid-range WPT for power grid monitoring equipment
  - Solution:
    - Planar PCB resonant winding
    - Multi-coil WPT system over insulation distance
- Challenge: Dynamic Modelling, load identification and Control
  - Solutions:
    - Dynamic Modeling Using Phasor Transformation
    - Dynamic Load Identification and Control

Challenge

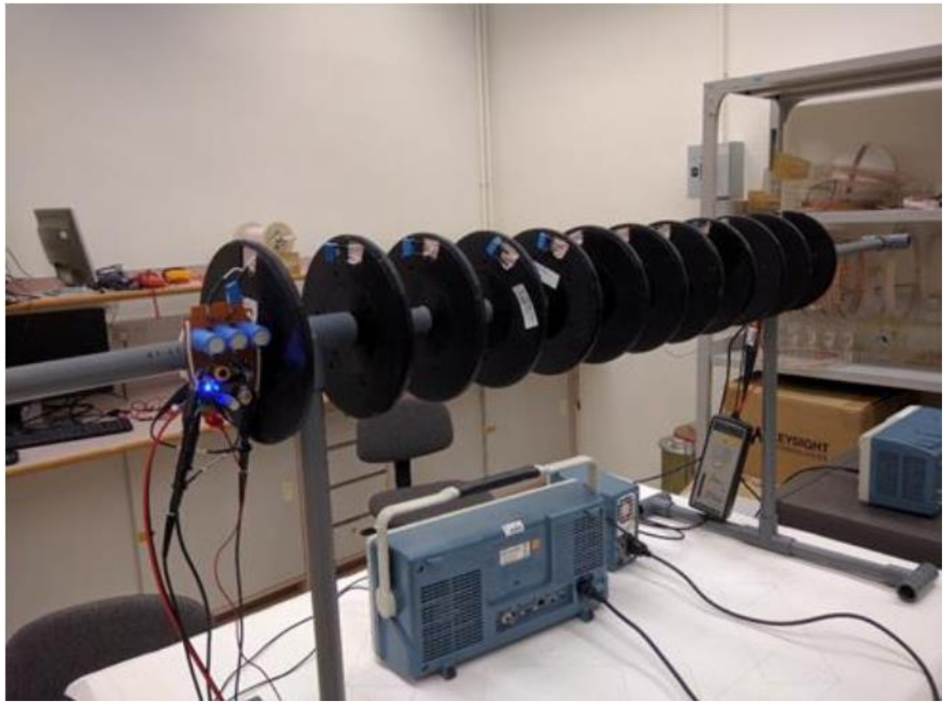

Multi-coil WPT system over 1.1 meter

[1] C. Zhang, D. Lin, N. Tang and S. Y. R. Hui, "A Novel Electric Insulation String Structure With High-Voltage Insulation and Wireless Power Transfer Capabilities," in IEEE Transactions on Power Electronics, vol. 33, no. 1, pp. 87-96, Jan. 2018.

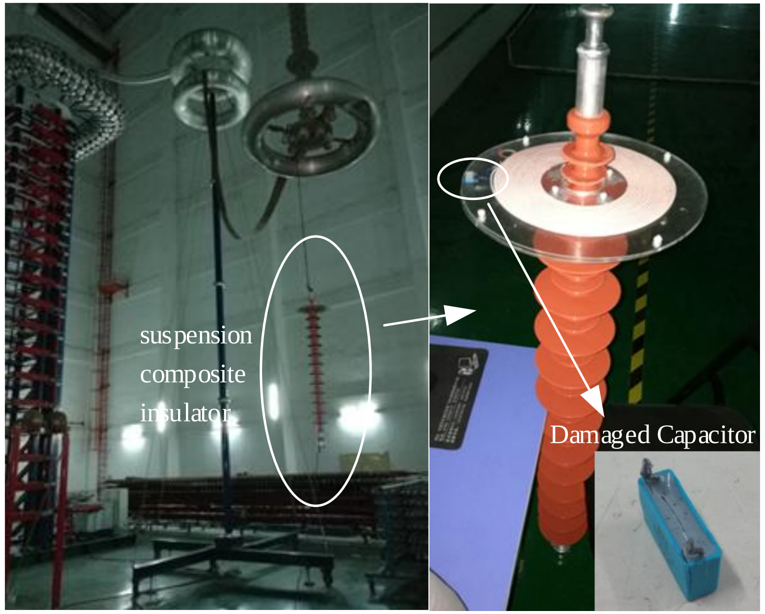

High Voltage Tests for Composite Insulators
-- China National Standard GB/T 19519-2014

No.	Test item	Standard requirement
B1	Power frequency dry withstand voltage test	Withstand voltage: 110 kV Tolerance time: 30 min
B2	Power frequency dry flashover test	Number of times: 5 times
B3	Power frequency dry withstand voltage test	Withstand voltage: 331 kV (80% of average flashover voltage) Tolerance time: 30 min
B4	Lightning impact dry withstand voltage test	Specified withstand voltage: 550 kV Actual withstand voltage: ≥ 619 kV Number of times: ±15 times

Outline

- Motivation
- Challenge: Mid-range WPT for power grid monitoring equipment
  - Solution:
    - Planar PCB resonant winding
    - Multi-coil WPT system over insulation distance
- Challenge: Dynamic Modelling, load identification and Control
  - Solutions:
    - Dynamic Modeling Using Phasor Transformation
    - Dynamic Load Identification and Control

Solution

Planar PCB Inductive Components

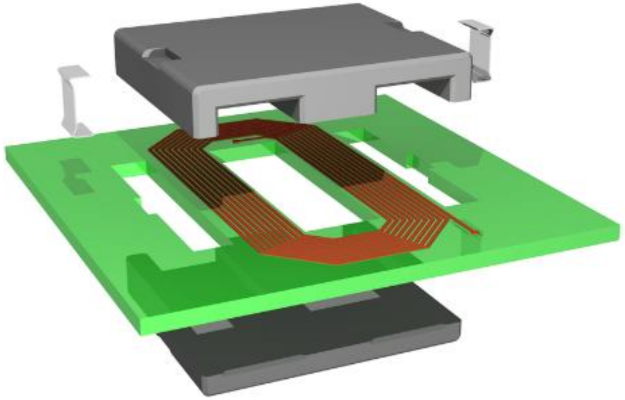

Inductors or Transformers
in both data and energy transmission

- Smaller size ✓
- Higher power density ✓
- Ease of manufacturing ✓
- Lower quality factor Q ✘

Research Objectives

- propose a planar PCB resonator to be embedded into insulators
- form a WPT system to provide energy for online monitoring devices

Planar PCB Resonator Design

Structure of the planar PCB resonator

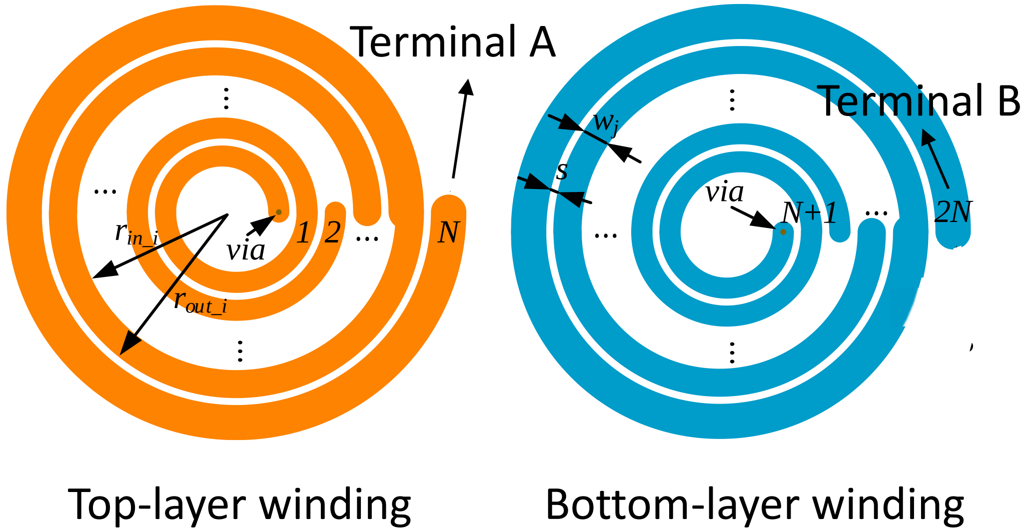

Plane view drawings of a PCB resonator

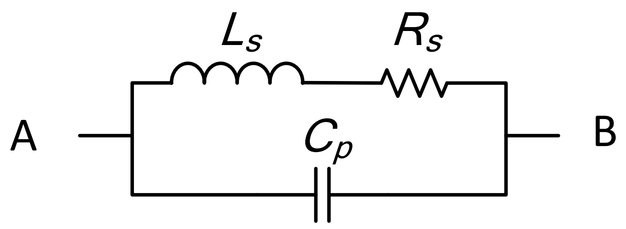

Lumped circuit model

L_S -- Self-inductance of the windings

C_P -- Parasitic capacitance between turns

R_S -- Series resistance of the windings

Parameters Calculation

Calculation of the Winding Inductance

$$L_S = \sum_{i=1}^{2N} \sum_{j=1}^{2N} \frac{\mu_0 \pi}{t_i t_j \ln\left(\frac{r_{out\_i}}{r_{in\_i}}\right) \ln\left(\frac{r_{out\_j}}{r_{in\_j}}\right)} \int_0^{\infty} S(kr_{out\_i}, kr_{in\_i}) \cdot S(kr_{out\_j}, kr_{in\_j}) Q(kt_i, kt_j) e^{-k|z_{ij}|} dk$$

$$Q(kx, ky) = \frac{2}{k^2}\left[\cosh k\frac{x+y}{2} - \cosh k\frac{x-y}{2}\right] \quad z > \frac{t_1 + t_2}{2}$$

$$S(kx, ky) = \frac{J_0(kx) - J_0(ky)}{k}$$

$$= \frac{2}{k}\left(t + \frac{e^{-kt} - 1}{k}\right) \quad z = 0, x = y = t$$

Calculation of the Parasitic Capacitance

$$E_{total} = \sum_{i=1}^{2N} \sum_{j=1}^{2N} \frac{1}{2} \frac{\varepsilon A_{ij}}{z_{ij}} \left[\frac{V_{A,ij}^2 + V_{A,ij} V_{B,ij} + V_{B,ij}^2}{3}\right]$$

$$C_P = \frac{2E_{total}}{V_L^2}$$

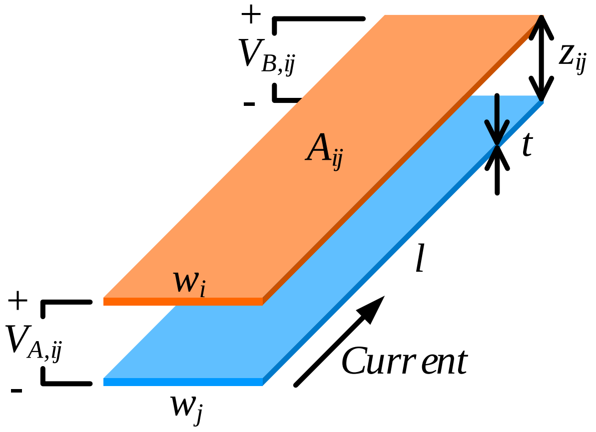

Parameters of copper traces for parasitic capacitance calculation.

Influence of the Winding Parameters

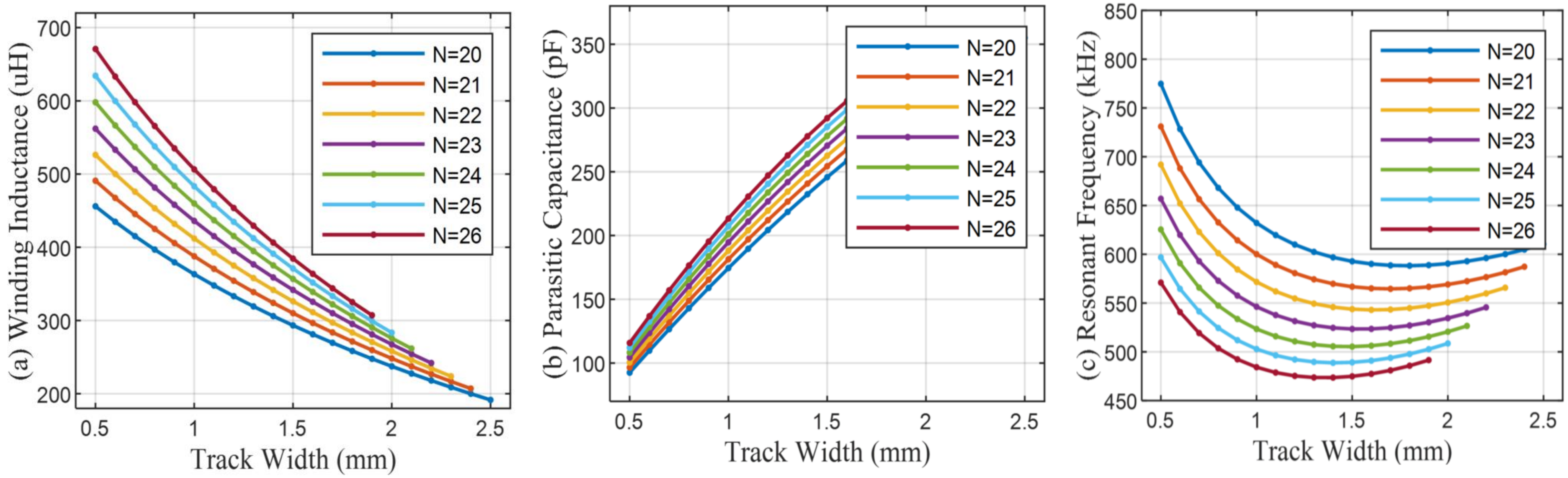

Characteristic of the PCB resonators. (Left) self-inductance L_S, (Middle) parasitic capacitance C_P and (Right) resonant frequency.

For a fixed track width

N $\uparrow \Rightarrow$ Winding Inductance $\uparrow$, Parasitic Capacitance $\uparrow$, Resonant Frequency $\downarrow$

For a fixed number of turns N

Track Width $\uparrow \Rightarrow$ Winding Inductance $\downarrow$, Parasitic Capacitance $\uparrow$, Resonant Frequency $\downarrow\uparrow$

Optimization of the quality factor Q

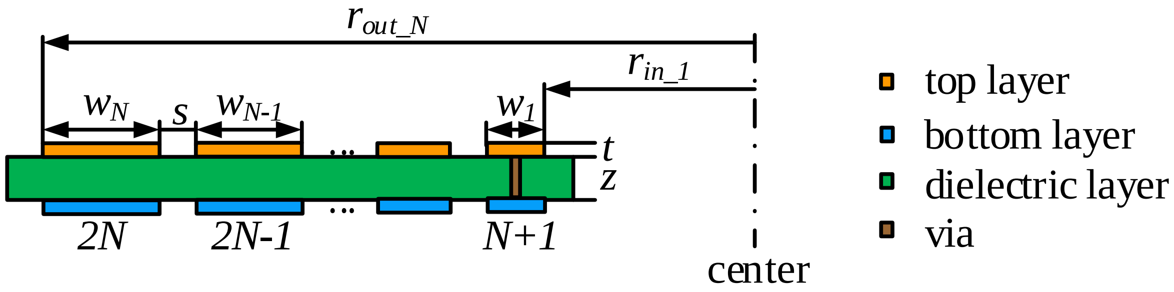

$$Q = \frac{\omega_r L_s}{R_s}$$

The cross-sectional view of a PCB resonator.

Hollow factor τ:

$\tau = r_{(in\_1)} \,/\, r_{(out\_N)}$

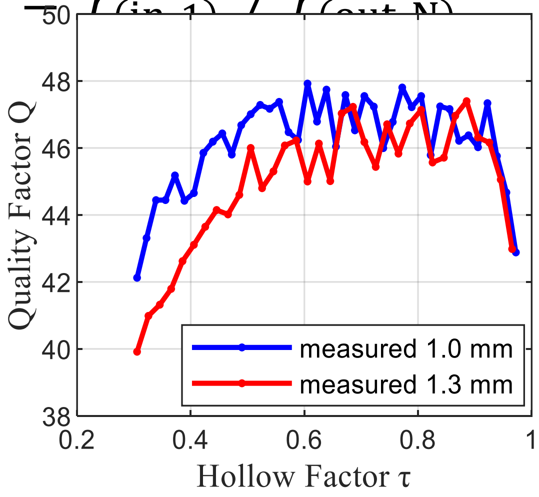

Q-factor against the hollow factor.

Trace-width-ratio σ:

$\sigma = w_n / w_{n-1}, n \in 2,3,\ldots,N$

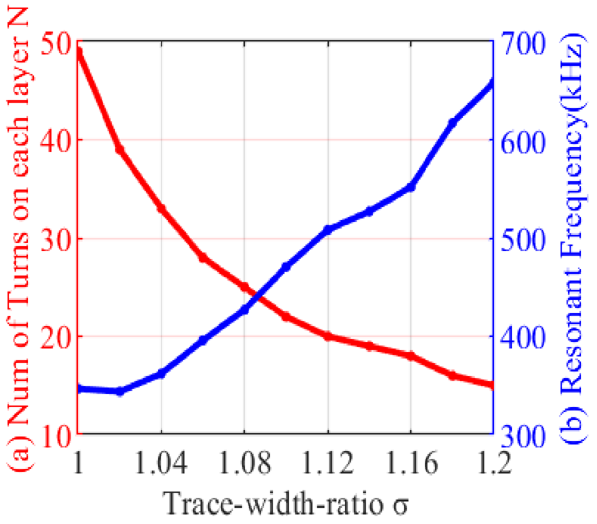

Relationship between trace-width-ratio σ and the maximum N and SRF of the PCB resonator.

Prototyping of PCB resonators

PCB resonators. (Left) double-layer winding. (Right) embedded in an insulator shed.

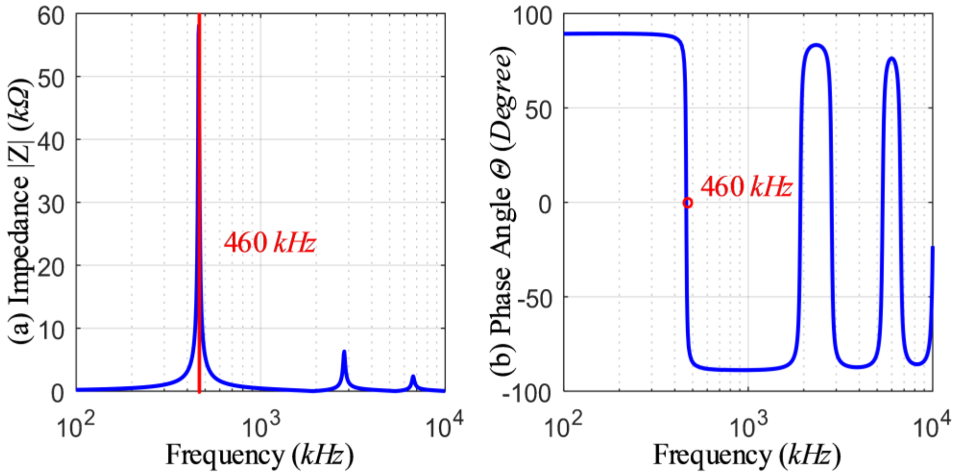

The frequency response of the PCB resonator.

PARAMETERS OF THE PCB RESONATORS

Parameters	Value
Outer radius r_{out_N}	100 mm
Inner diameter r_{in_1}	50 mm
Hollow factor τ	0.5
Thickness of PCB board z	1.6 mm
Material and dielectric constant of PCB	FR4, 4.1
Thickness of copper traces t	140 µm
Trace width of innermost trace w_1	0.5 mm
Trace width of median trace w_{median}	1.18
Trace width of outer most trace w_N	3.5 mm
Trace width ratio σ	1.1
Clearance between copper traces s	0.5 mm
Number of turn on each layer N	22
Winding inductance L_S	321 µH
Self-capacitance C_P	369 pF
Self-resonant frequency SRF	460 kHz
AC resistance R_S at SRF	15 Ω
Quality factor Q at SRF	64

Outline

- Motivation
- Challenge: Mid-range WPT for power grid monitoring equipment
  - Solution:
    - Planar PCB resonant winding
    - Multi-coil WPT system over insulation distance
- Challenge: Dynamic Modelling, load identification and Control
  - Solutions:
    - Dynamic Modeling Using Phasor Transformation
    - Dynamic Load Identification and Control

System Configuration

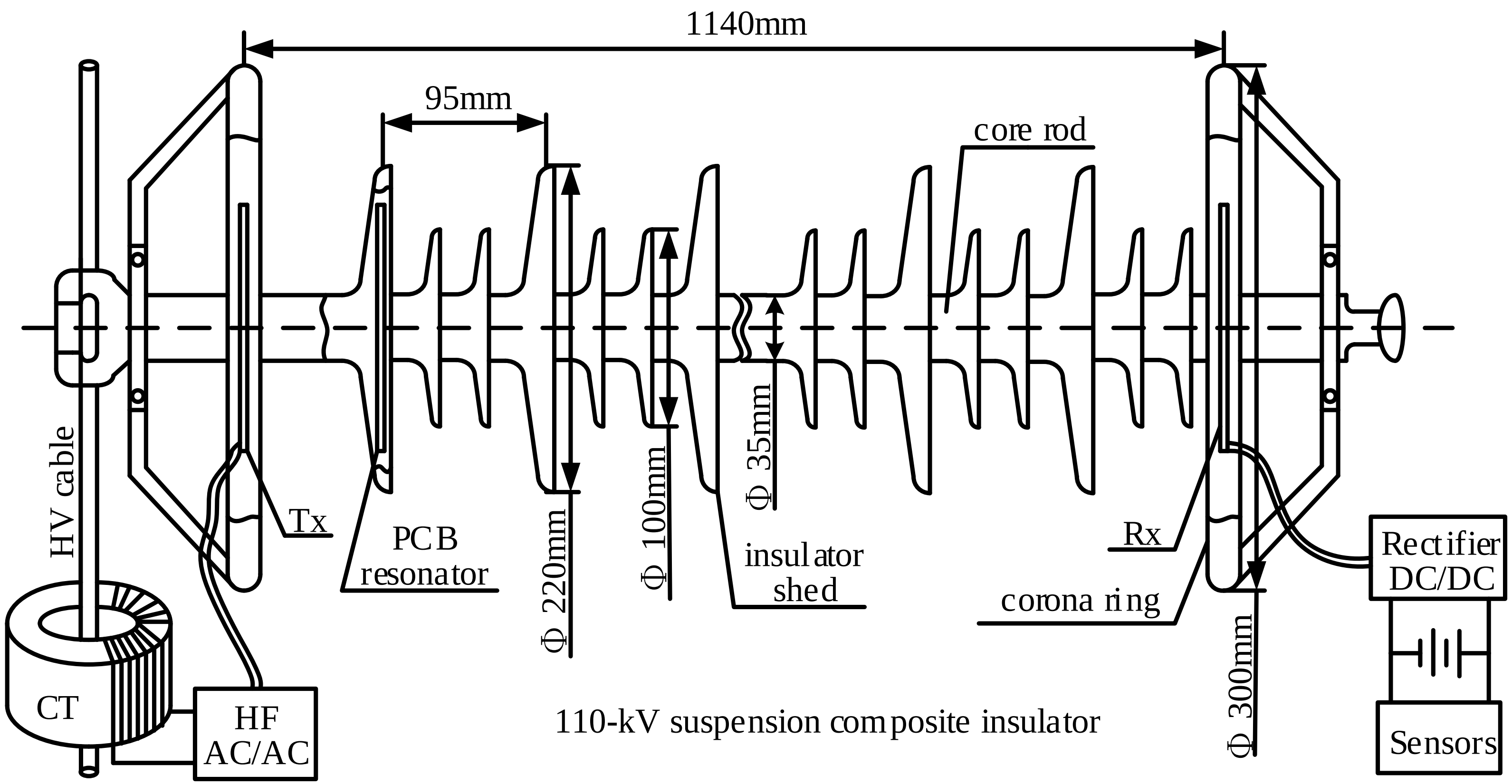

Physical dimensions of a 110-kV suspension type composite insulator model: FXBW -110/120-1340

Prototype of the High-Voltage Insulator with WPT Capability

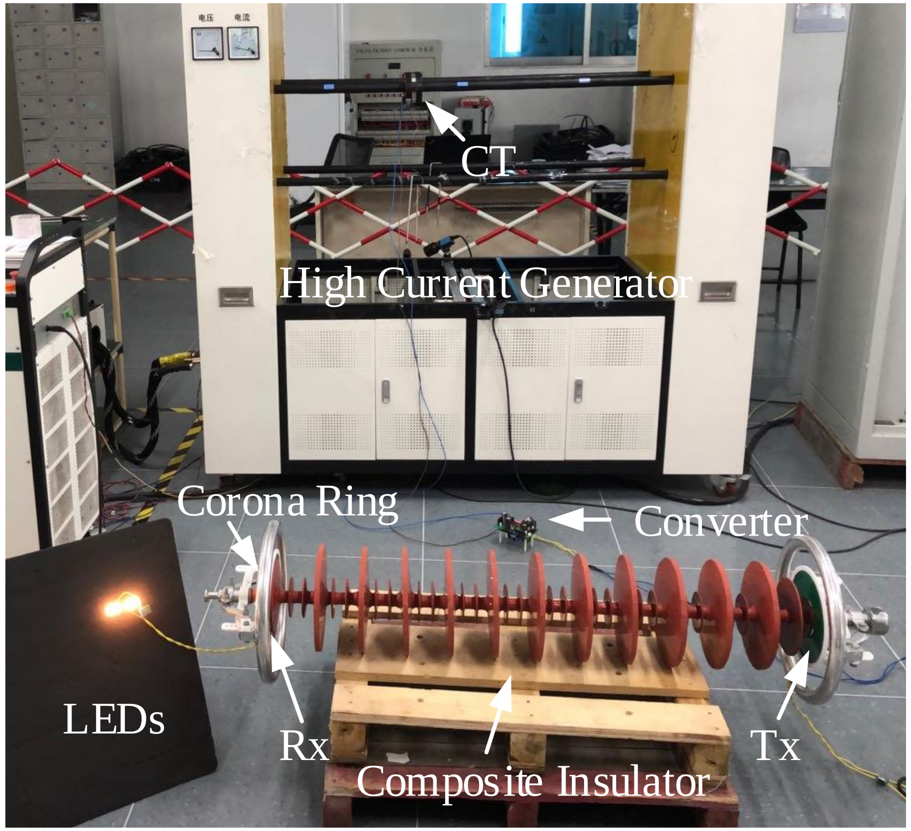

Experimental setup in laboratory.

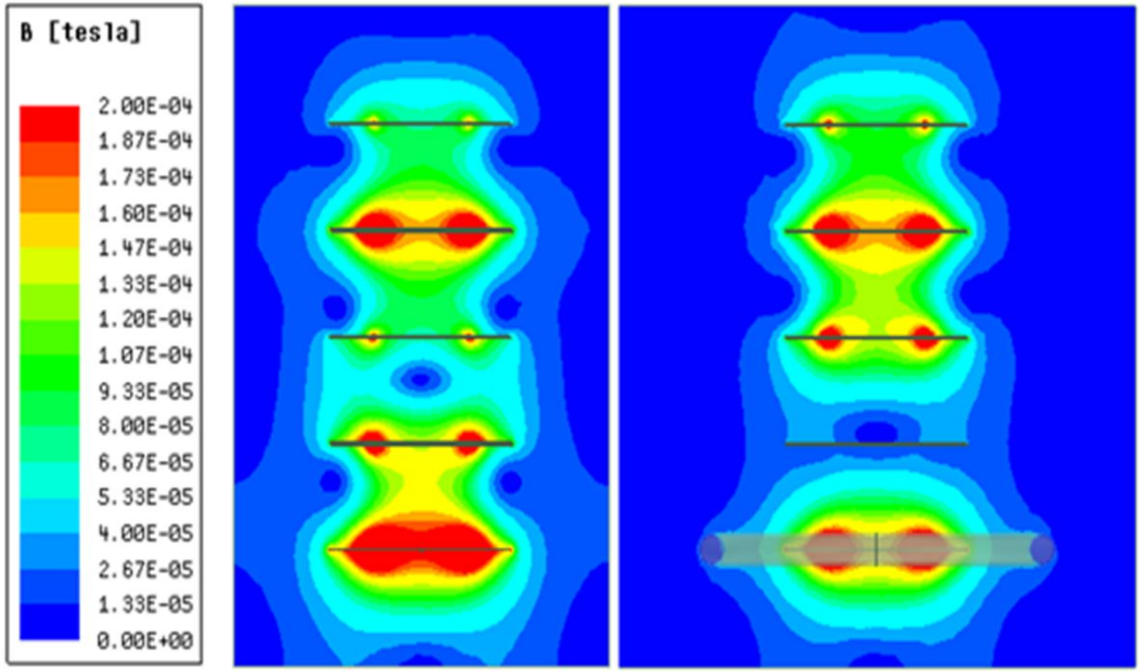

Magnetic field distribution of domino-resonator WPT systems. (Left): without alloy corona ring, and (Right) with alloy corona ring.

[1] J. Qu, L. He, N. Tang and C.-K. Lee, "Wireless Power Transfer Using Domino-Resonator for 110-kV Power Grid Online Monitoring Equipment," in IEEE Transactions on Power Electronics, vol. 35, no. 11, pp. 11380-11390, Nov. 2020.

Modeling of the Multi-Coil WPT System

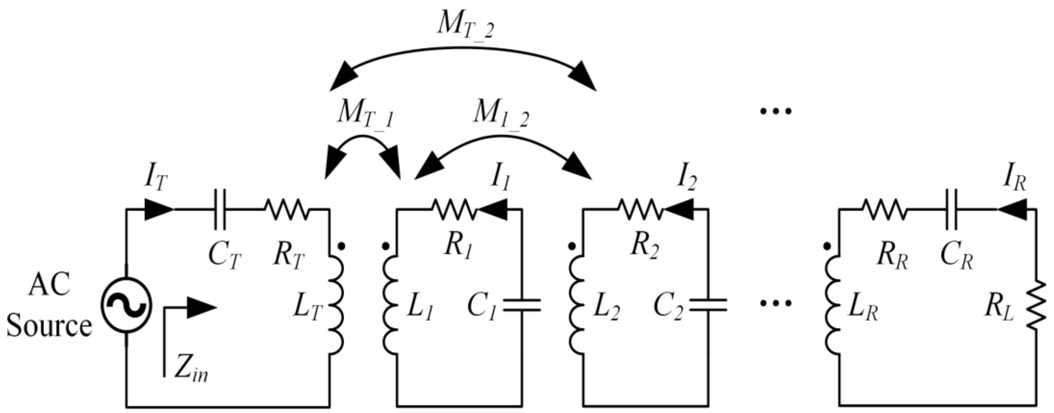

Schematic of domino-resonator WPT system

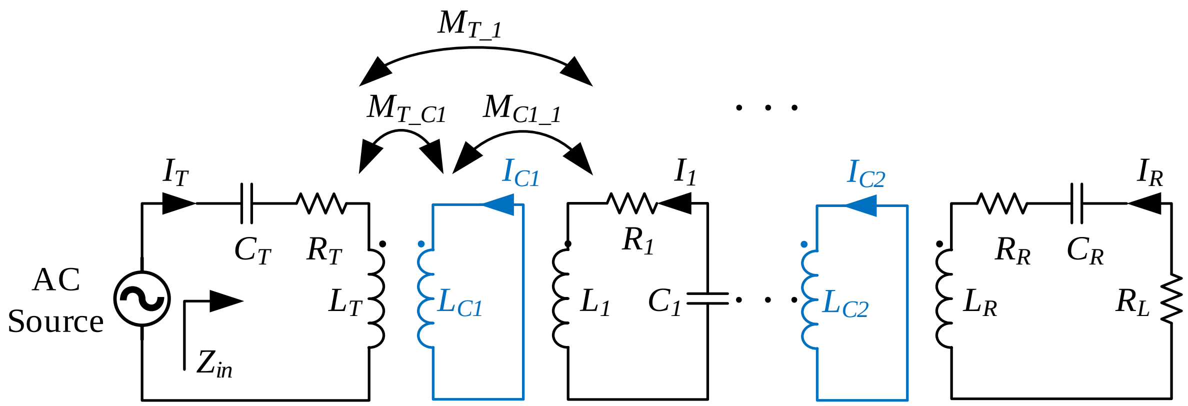

Schematic of a domino-resonator WPT with corona rings

$$\begin{bmatrix} V_S \\ 0 \\ \vdots \\ 0 \\ 0 \end{bmatrix} = \begin{bmatrix} Z_T & j\omega M_{T\_1} & \cdots & j\omega M_{T\_11} & j\omega M_{T\_R} \\ j\omega M_{1\_T} & Z_1 & \cdots & j\omega M_{1\_11} & j\omega M_{1\_R} \\ \vdots & \vdots & \ddots & \vdots & \vdots \\ j\omega M_{11\_T} & j\omega M_{11\_2} & \cdots & Z_{11} & j\omega M_{11\_R} \\ j\omega M_{R\_T} & j\omega M_{11\_2} & \cdots & j\omega M_{R\_11} & Z_R + R_L \end{bmatrix} \begin{bmatrix} I_T \\ I_1 \\ \vdots \\ I_{11} \\ I_R \end{bmatrix}$$

$$\begin{bmatrix} V_S \\ 0 \\ 0 \\ \vdots \\ 0 \\ 0 \end{bmatrix} = \begin{bmatrix} Z_T & j\omega M_{T\_C1} & j\omega M_{T\_1} & \cdots & j\omega M_{T\_C2} & j\omega M_{T\_R} \\ j\omega M_{C1\_T} & j\omega L_{C1} & j\omega M_{C1\_1} & \cdots & j\omega M_{C1\_C2} & j\omega M_{C1\_R} \\ j\omega M_{1\_T} & j\omega M_{1\_C1} & Z_1 & \cdots & j\omega M_{1\_C2} & j\omega M_{1\_R} \\ & \vdots \quad \vdots & \vdots & \ddots & \vdots & \vdots \\ j\omega M_{C2\_T} & j\omega M_{C2\_C1} & j\omega M_{C2\_1} & \cdots & j\omega L_{C2} & j\omega M_{C2\_R} \\ j\omega M_{R\_T} & j\omega M_{R\_C2} & j\omega M_{R\_1} & \cdots & j\omega M_{R\_C2} & Z_R + R_L \end{bmatrix} \begin{bmatrix} I_T \\ I_{C1} \\ I_1 \\ \vdots \\ I_{C2} \\ I_R \end{bmatrix}$$

$$Z_i = R_i + j(\omega L_i - \frac{1}{\omega C_i})$$

$$P_{out} = I_R^2 R_L$$

$$\eta = \frac{I_R^2 R_L}{I_T^2 R_T + \sum_{i=1}^{11} I_i^2 R_i + I_R^2 R_R + I_R^2 R_L}$$

$$L_C = 505 \text{ nH}$$

$$\mathrm{Im} Z_R = \frac{\omega^2 M_{T\_C1}^2}{j\omega L_C}$$

Selected Experimental Results

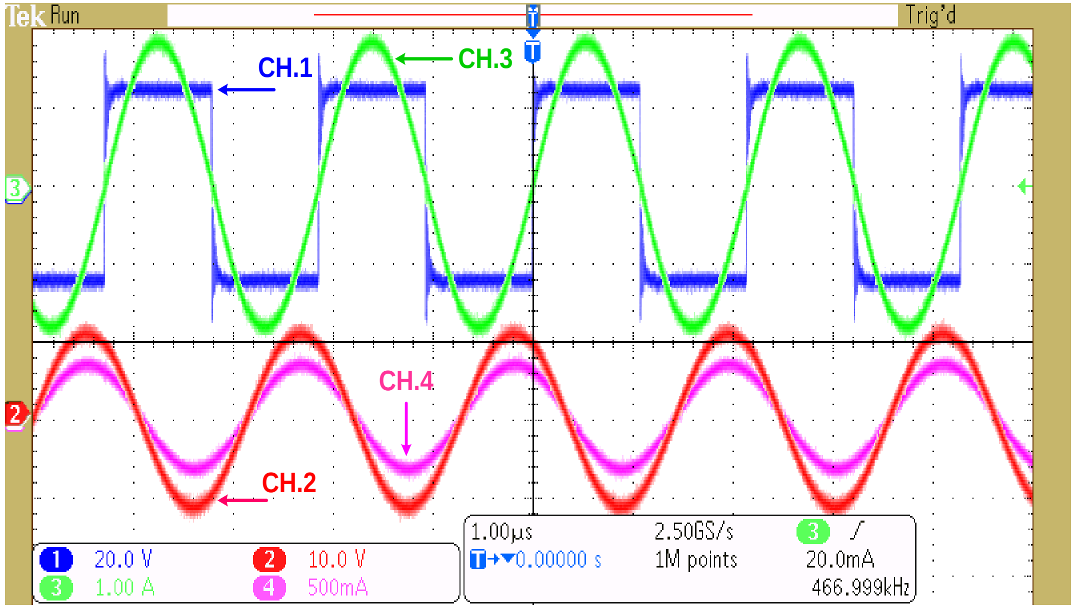

Measured waveforms of the domino-resonator WPT system. Timebase = 1μS/Div.

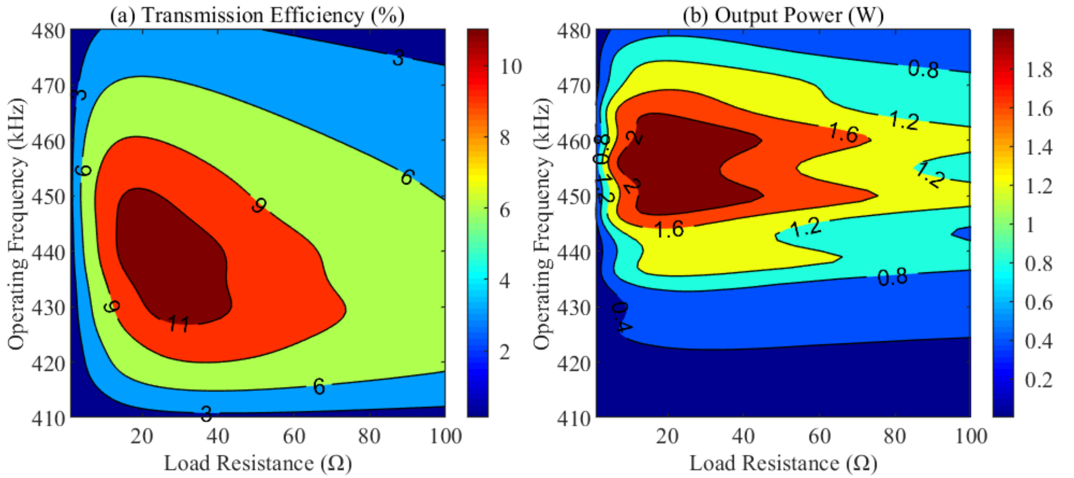

Computed transmission efficiency and output power

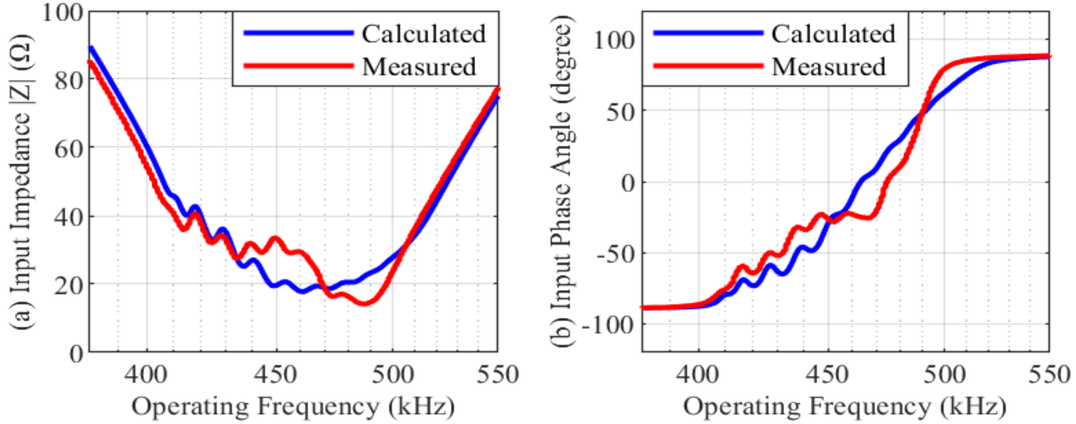

Measured and calculated input impedance measured by network analyzer.

Outline

- Motivation
- Challenge: Mid-range WPT for power grid monitoring equipment
  - Solution:
    - Planar PCB resonant winding
    - Multi-coil WPT system over insulation distance
- Challenge: Dynamic Modelling, load identification and Control
  - Solutions:
    - Dynamic Modeling Using Phasor Transformation
    - Dynamic Load Identification and Control

System Configuration

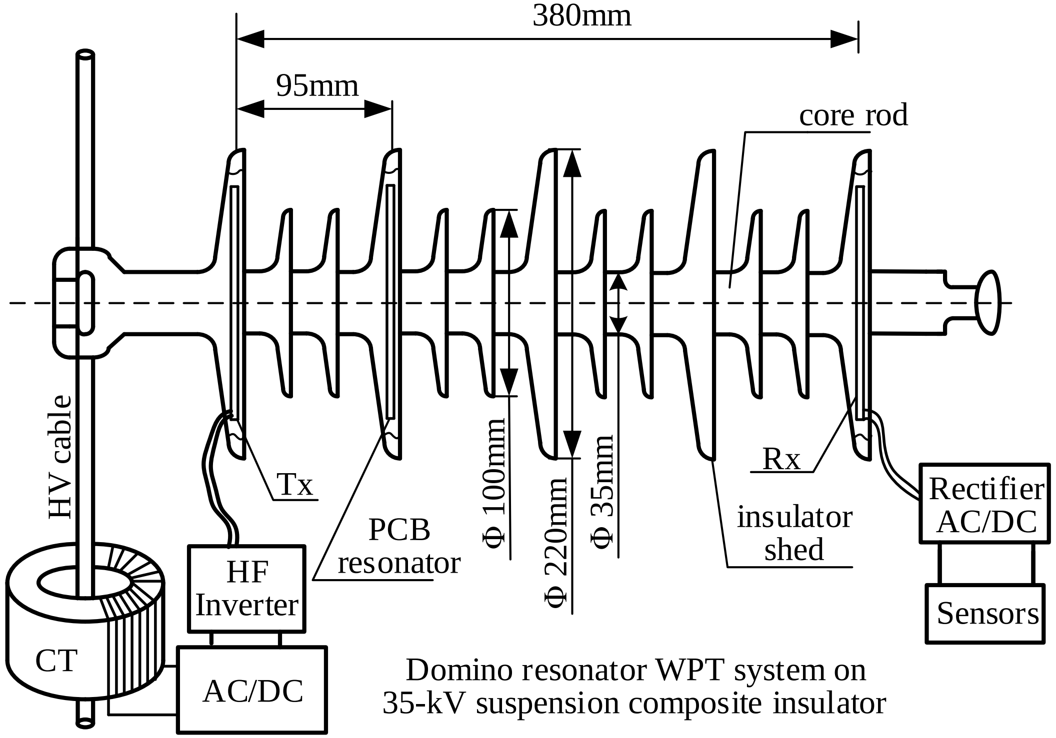

Configuration of 35-kV suspension type composite insulator

Operating Characteristic of Online Monitoring Equipment

Rated input voltage: 12V		
Operation Mode	Power Consumption	Equivalent Load
Sleeping mode	3 W	48 Ω
Data collecting mode	12 W	12 Ω

Control Schemes of WPT System

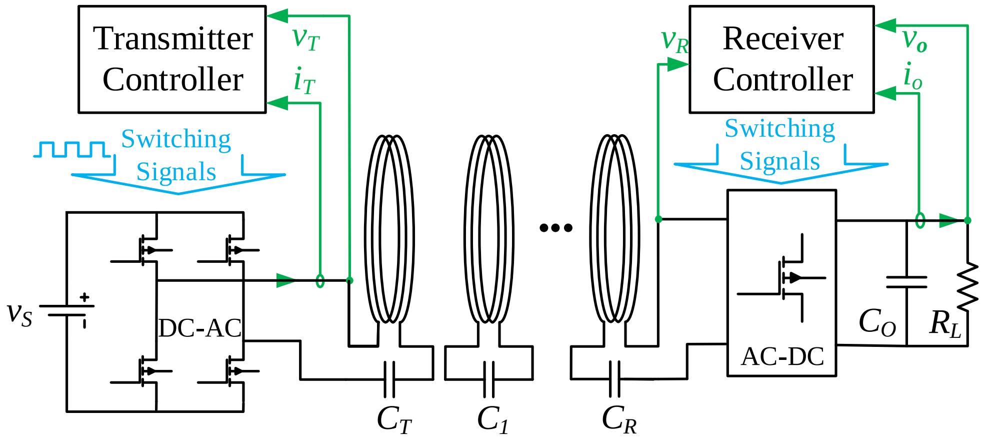

(a) Separate control scheme on transmitter and receiver side

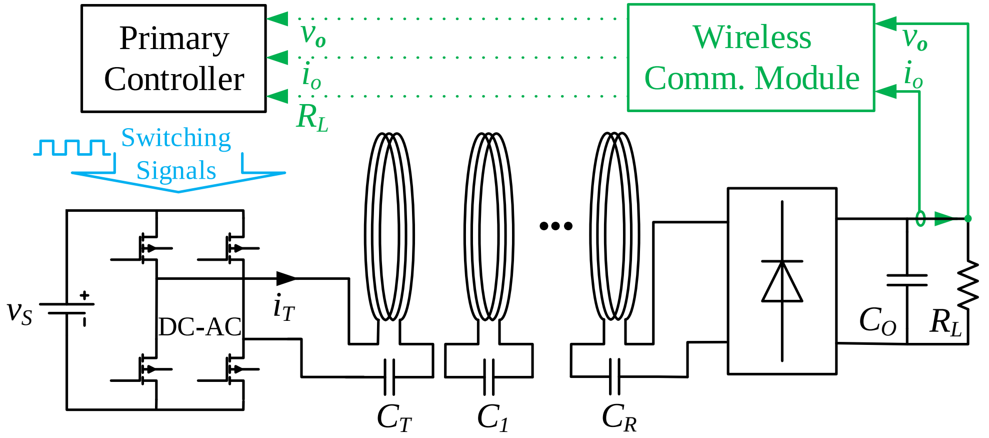

(b) Primary control scheme with wireless feedback information

Control methods for output voltage regulation

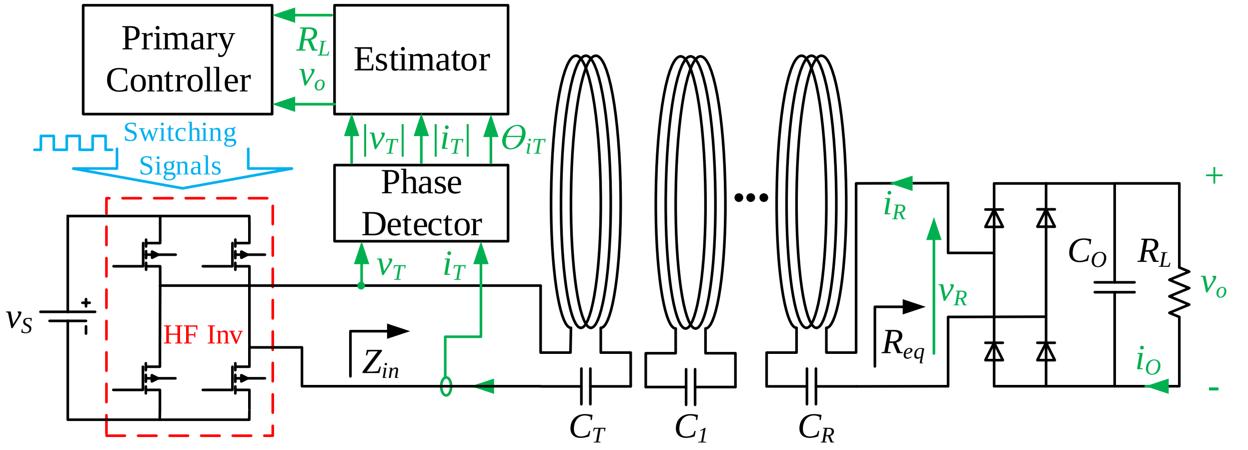

Primary control scheme without wireless feedback from receiver side

- Lower cost ✓
- Higher efficiency ✓
- Higher flexibility ✓
- Steady state only ✗

Existing load identification results

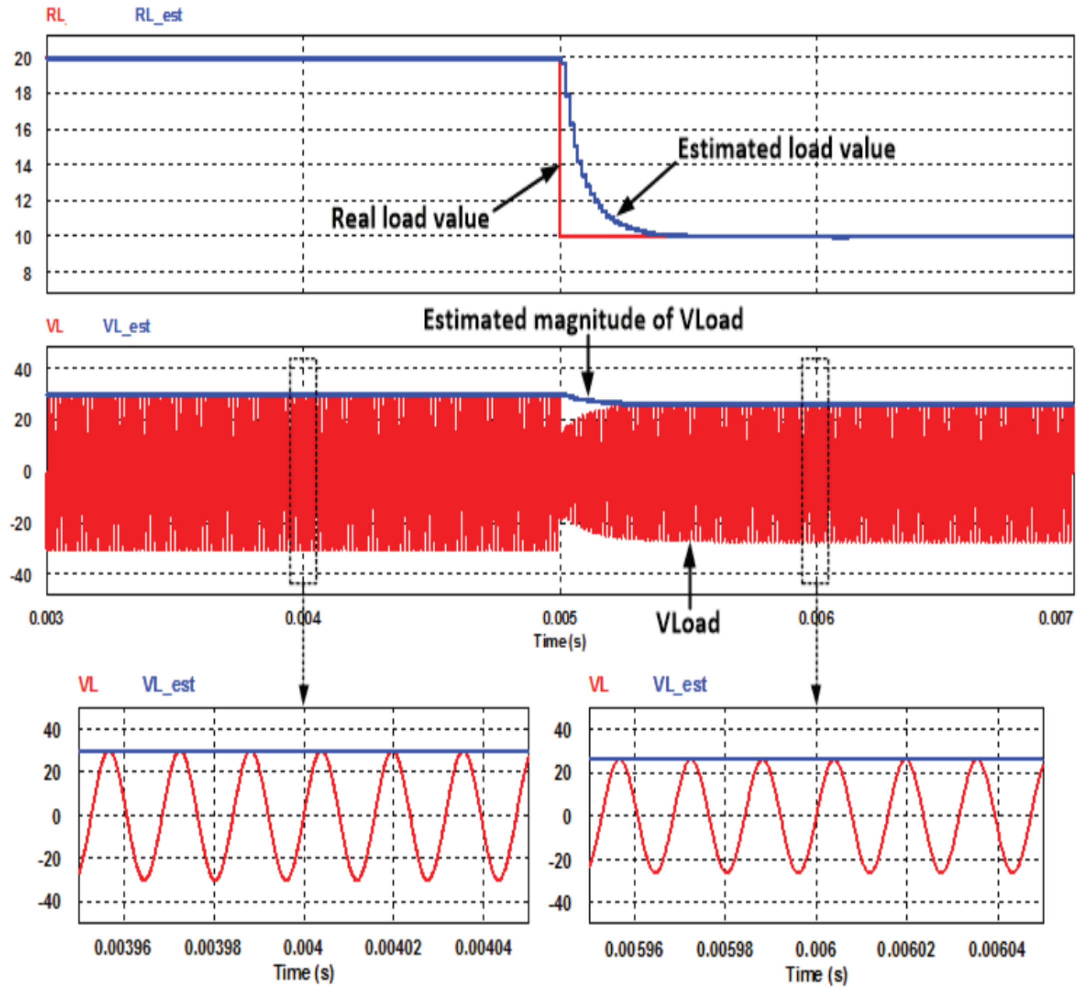

Load monitoring for SP compensated IPT system

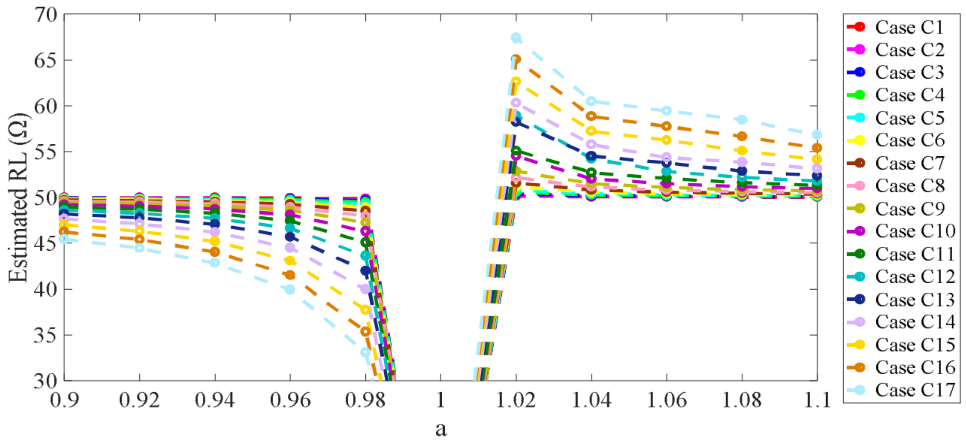

Frequency-Sweep Based Load Monitoring

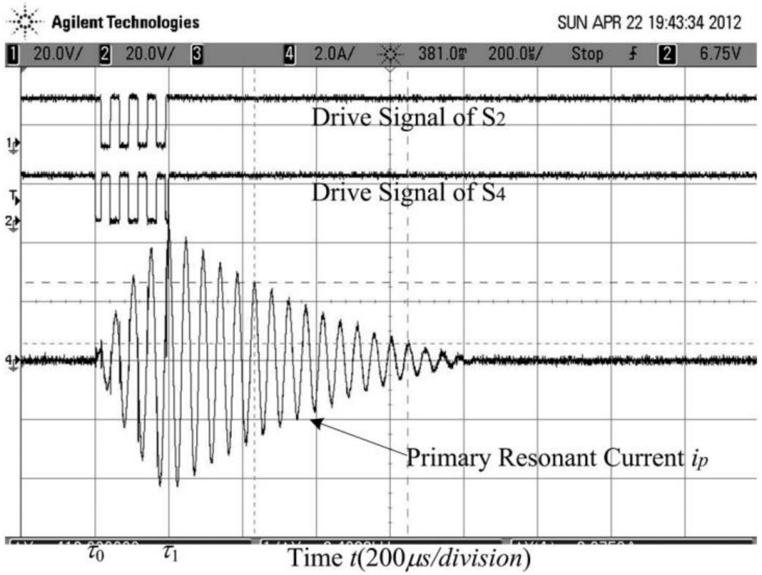

Energy Injection Based Load Monitoring

Outline

- Motivation
- Challenge: Mid-range WPT for power grid monitoring equipment
  - Solution:
    - Planar PCB resonant winding
    - Multi-coil WPT system over insulation distance
- Challenge: Dynamic Modelling, load identification and Control
  - Solutions:
    - Dynamic Modeling Using Phasor Transformation
    - Dynamic Load Identification and Control

Phasor Transformation Method

Traditional Euler's formula

$$A\cos(\omega t+\theta) = A\frac{e^{j(\omega t+\theta)}+e^{-j(\omega t+\theta)}}{2} = \mathrm{Re}\{Ae^{j(\omega t+\theta)}\} = \mathrm{Re}\{Ae^{j\theta}e^{j\omega t}\}$$

Modified for transient state $x(t) = \mathrm{Re}[\boldsymbol{x}(t)e^{j\omega t}]$

Apply on the circuit elements, find their equivalent model

$$V_L(t) = e^{-j\omega_s t}Re^{-1}[v_L(t)] = e^{-j\omega_s t}Re^{-1}\left[L\frac{di_L(t)}{dt}\right]$$

$$= e^{-j\omega_s t}Re^{-1}\left[L\frac{dRe[e^{j\omega_s t}I_L(t)]}{dt}\right]$$

$$= Le^{-j\omega_s t}Re^{-1}\left[Re[j\omega_S I_L(t)e^{j\omega_s t}+\frac{dI_L(t)}{dt}e^{j\omega_s t}]\right]$$

$$= j\omega_S L I_L(t) + L\frac{dI_L(t)}{dt}$$

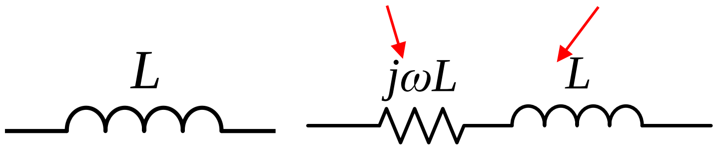

Time domain Phasor domain

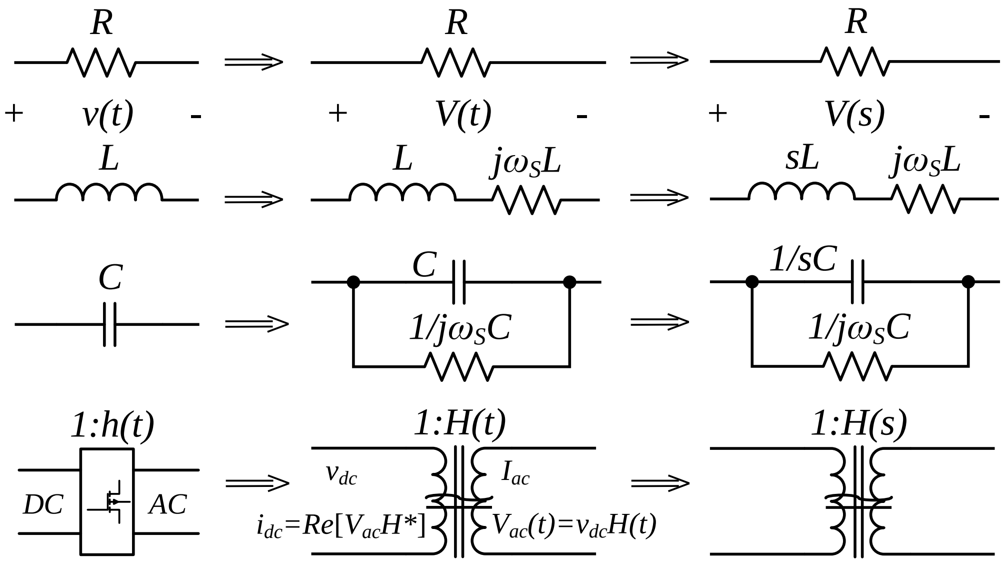

The circuit elements in the time domain (left), phasor domain (middle) and frequency domain (right)

Dynamic Circuit Model

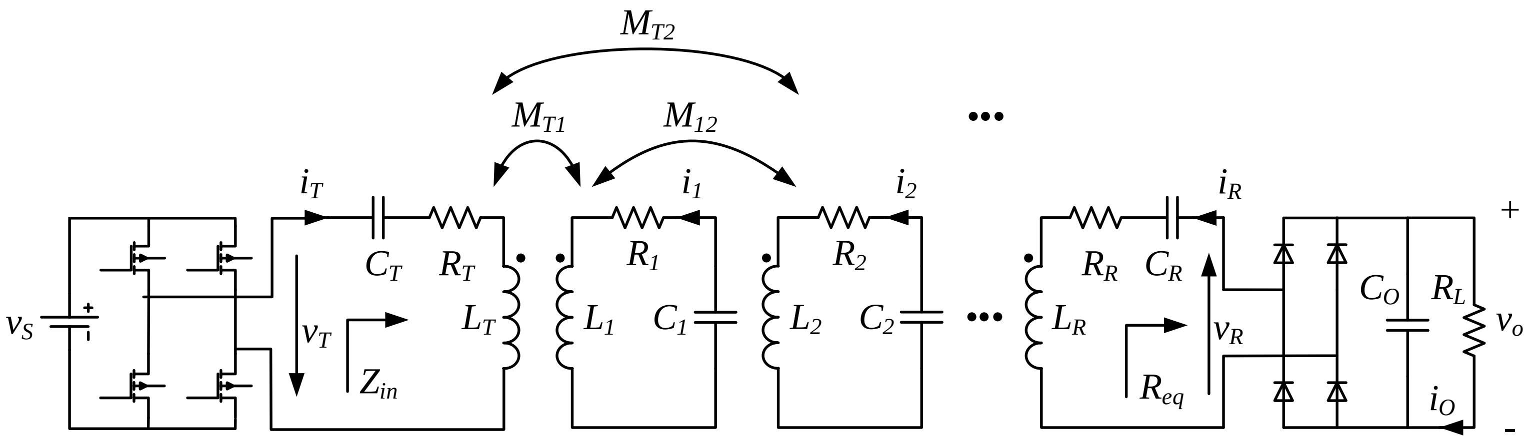

Schematic of a domino-resonator WPT system.

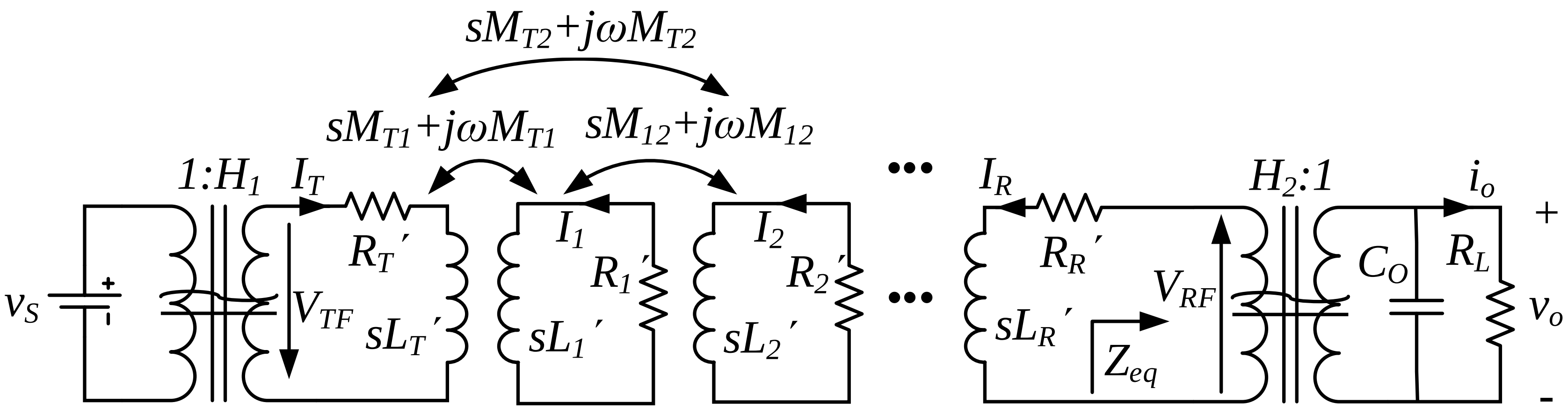

The domino-resonator WPT system in the frequency domain

Modelling the Components in WPT System

Modeling the inverter and rectifier

$$v_{TF}(t) = \frac{4v_S}{\pi} \sin(\pi D)\cos(\omega_S t) = h_1(t)v_S$$

$$v_{RF}(t) = \frac{4v_O}{\pi}\cos(\omega_S t + \Theta_{h2}) = h_2(t)v_O$$

$$\begin{aligned}
i_O &= h_2(t)i_R(t) \\
&= |h_2(t)|\cos(\omega_S t + \Theta_{h2})\,|i_R(t)|\cos(\omega_S t + \Theta_{iR}) \\
&= \frac{|h_2(t)||i_R(t)|}{2} + |h_2(t)||i_R(t)|\cos(2\omega_S t + 2\Theta_{iR}) \\
&= \frac{|h_2(t)||i_R(t)|}{2}
\end{aligned}$$

$$R_{eq} = \frac{8}{\pi^2}R_L$$

Simplification of the resonant circuit

$$\begin{aligned}
Z_{LC} &= sL + j\omega_S L + \frac{1}{sC + j\omega_S C} \\
&= \frac{(s + j\omega_S + j\omega_r)(s + j\omega_S - j\omega_r)}{s + j\omega_S} \\
&\approx \frac{(j\omega_S + j\omega_r)(s + j\omega_S - j\omega_r)}{j\omega_S} \\
&= s\frac{\omega_S + \omega_r}{\omega_S}L + j\frac{\omega_S^2 - \omega_r^2}{\omega_S}L \\
&= sL' + j\Delta\omega L'
\end{aligned}$$

Dynamic Model of the WPT system

$$\begin{bmatrix} v_S(s)H_1(s) \\ 0 \\ \vdots \\ 0 \\ 0 \end{bmatrix} = \begin{bmatrix} R'_T + sL'_T & j\omega M_{T1} + sM_{T1} & \cdots & j\omega M_{TR} + sM_{TR} & 0 \\ j\omega M_{1T} + sM_{1T} & R'_1 + sL'_1 & \cdots & j\omega M_{1R} + sM_{1R} & 0 \\ \vdots & \vdots & \ddots & \vdots & \vdots \\ j\omega M_{RT} + sM_{RT} & j\omega M_{R1} + sM_{R1} & \cdots & R'_R + sL'_R & 1 \\ 0 & 0 & \cdots & -8/\pi^2 & sC_o + \frac{1}{R_L} \end{bmatrix} \begin{bmatrix} I_T(s) \\ I_1(s) \\ \vdots \\ I_R(s) \\ H_2(s)v_o(s) \end{bmatrix}$$

$$\underbrace{\begin{bmatrix} 1 \\ 0 \\ \vdots \\ 0 \\ 0 \end{bmatrix}}_{M} v_S H_1 = \underbrace{\begin{bmatrix} R'_T & j\omega M_{T1} & \cdots & j\omega M_{TR} & 0 \\ j\omega M_{1T} & R'_1 & \cdots & j\omega M_{1R} & 0 \\ \vdots & \vdots & \ddots & \vdots & \vdots \\ j\omega M_{RT} & j\omega M_{R1} & \cdots & R'_R & 1 \\ 0 & 0 & \cdots & -8/\pi^2 & \frac{1}{R_L} \end{bmatrix}}_{P} \underbrace{\begin{bmatrix} I_T \\ I_1 \\ \vdots \\ I_R \\ H_2 v_o \end{bmatrix}}_{X} + \underbrace{\begin{bmatrix} L'_T & M_{T1} & \cdots & M_{TR} & 0 \\ M_{1T} & L'_1 & \cdots & M_{1R} & 0 \\ \vdots & \vdots & \ddots & \vdots & \vdots \\ M_{RT} & M_{R1} & \cdots & L'_R & 0 \\ 0 & 0 & \cdots & 0 & C_o \end{bmatrix}}_{Q} \underbrace{\begin{bmatrix} \dot{I}_T \\ \dot{I}_1 \\ \vdots \\ \dot{I}_R \\ H_2 \dot{v}_o \end{bmatrix}}_{\dot{X}}$$

$$\begin{cases} \dot{X} = AX + Bv_S H_1 \\ Y = CX \end{cases}$$

$$A = -Q^{-1}P, B = Q^{-1}M$$

Transfer Function:

$$G(s) = C(sI - A)^{-1}B + C(sI - A)^{-1}X_0$$

Experiment Setup

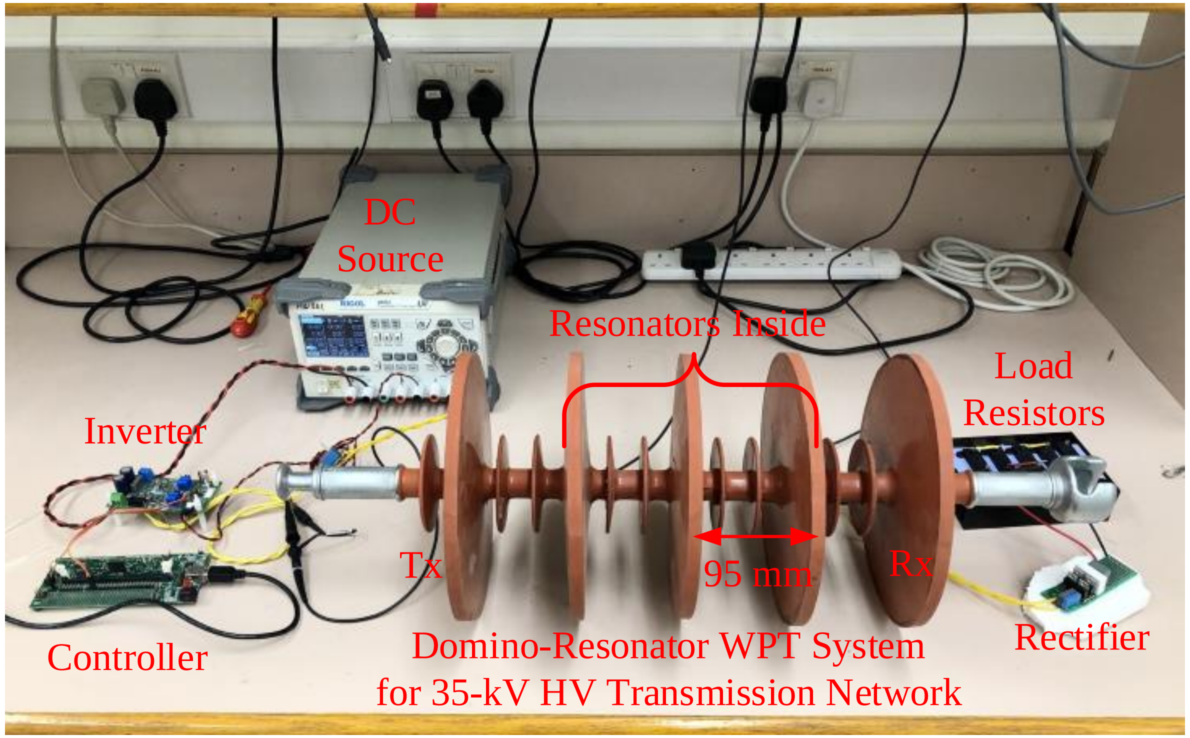

Experiment platform for domino-resonator WPT

PARAMETERS OF THE PCB RESONATORS

Parameters	Value
The inductance of the resonators $L_i, i = 1,2,3$	320 uH
Self-capacitance of resonators C_p	344 pF
Self-resonant frequency of resonators f_r	480 kHz
AC resistance R_i of resonators near f_r	25 Ω
The inductance of the Tx and Rx coil	82 uH
Compensation capacitor for Tx/Rx coil C_T, C_R	1.33 nF
AC resistance of Tx/Rx coil near F_r, R_T, R_R	4 Ω
Filter capacitor C_o	846 nF

[1] J. Qu and C. -K. Lee, "Dynamic Modeling for the Wireless Power Transfer System in Domino Structure," in IEEE Transactions on Industrial Electronics, vol. 69, no. 4, pp. 3556-3565, April 2022.

Static Results

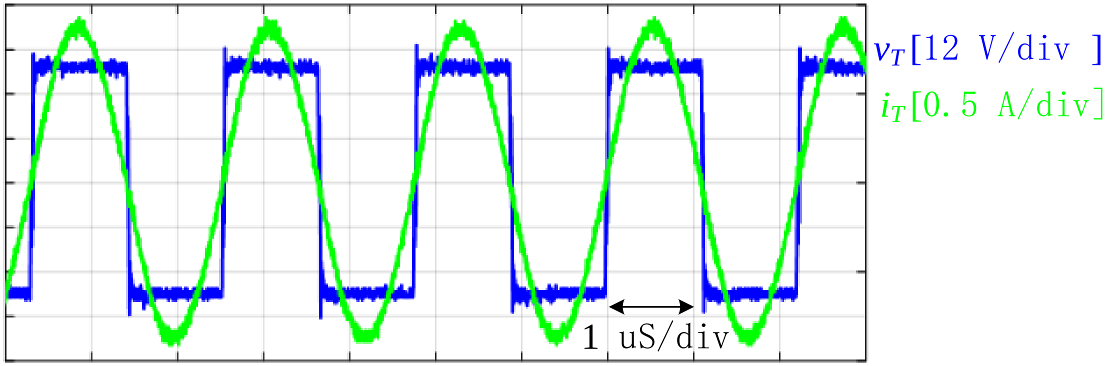

(a) Input waveforms

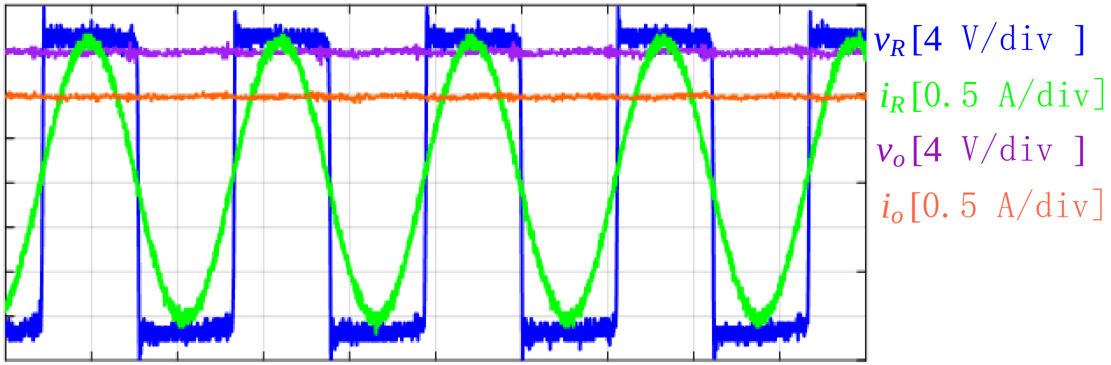

(b) Output waveforms

Steady-state voltage and current waveforms at the (a) transmitter coil and (b) receiver coil when the load resistance is 12 *Ω*

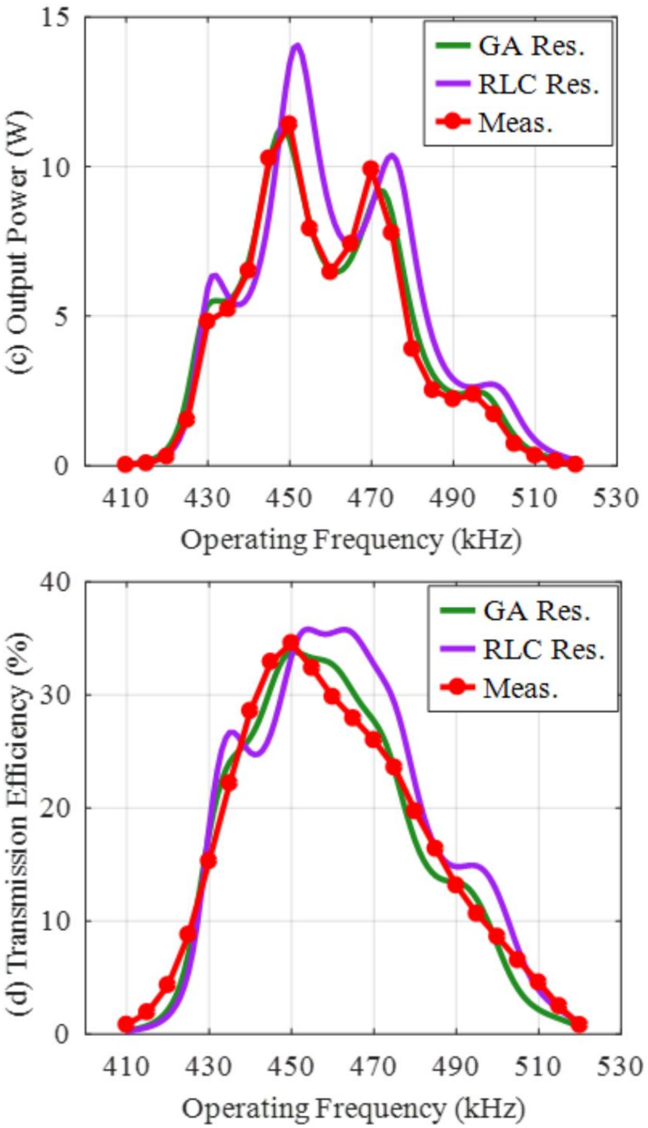

Comparison of the measured and calculated output power (left) and transmission efficiency (right) under steady-state condition.

Dynamic Results

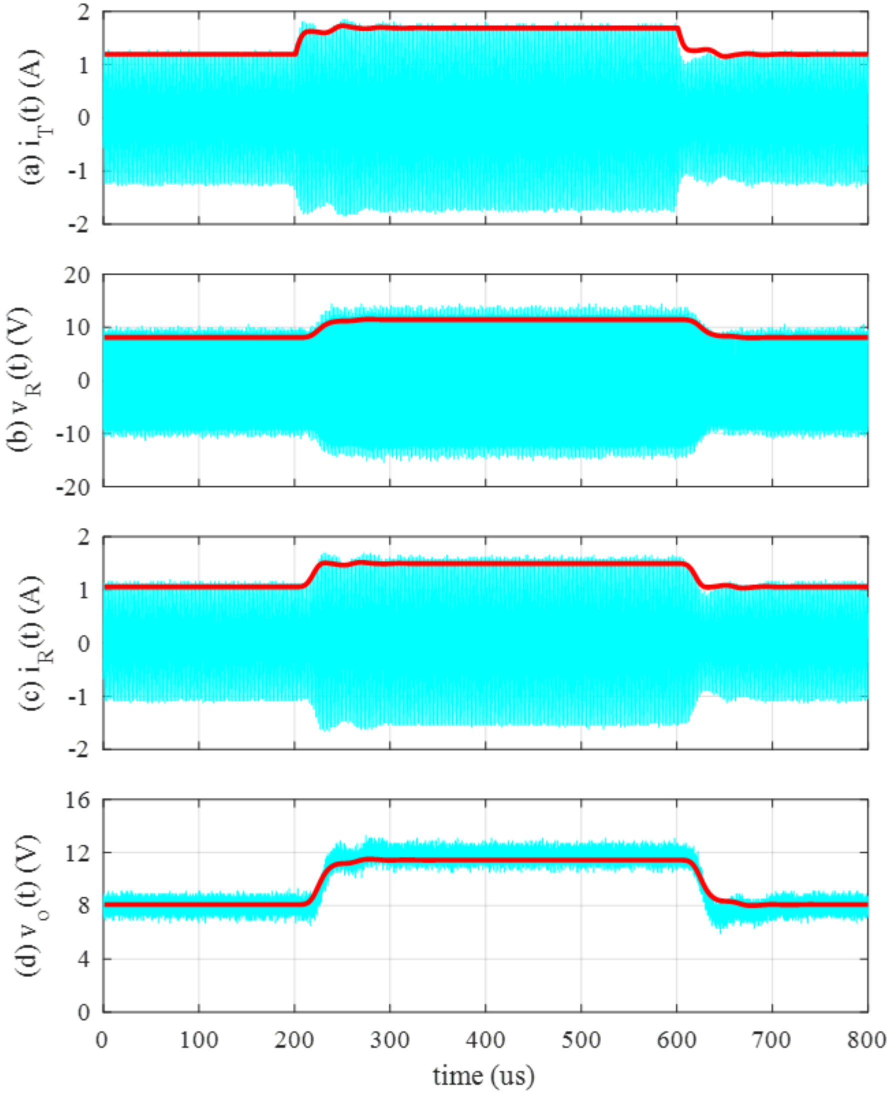

Input voltage step changes

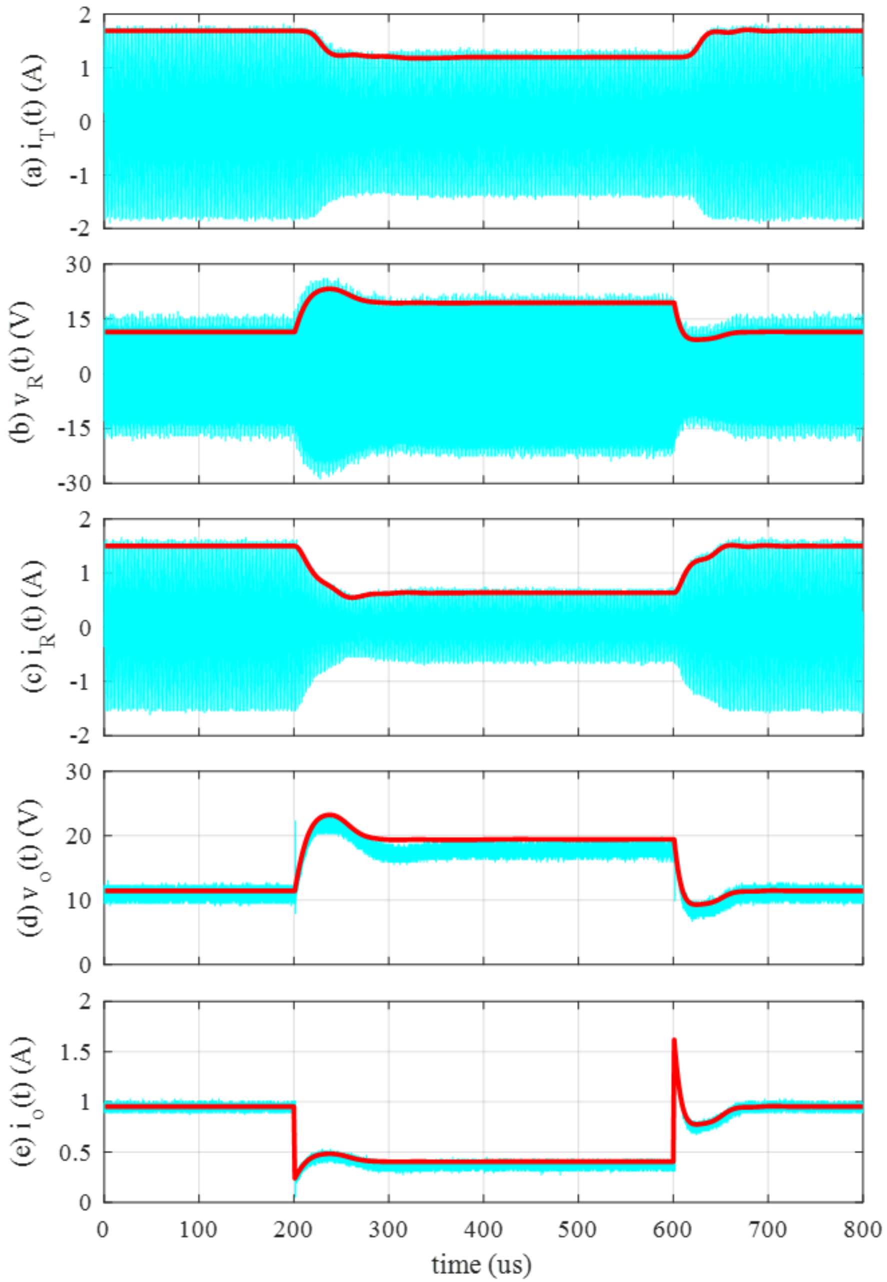

Load step changes

Outline

- Motivation
- Challenge: Mid-range WPT for power grid monitoring equipment
    - Solution:
        - Planar PCB resonant winding
        - Multi-coil WPT system over insulation distance
- Challenge: Dynamic Modelling, load identification and Control
    - Solutions:
        - Dynamic Modeling Using Phasor Transformation
        - Dynamic Load Identification and Control

Dynamic Load Identification

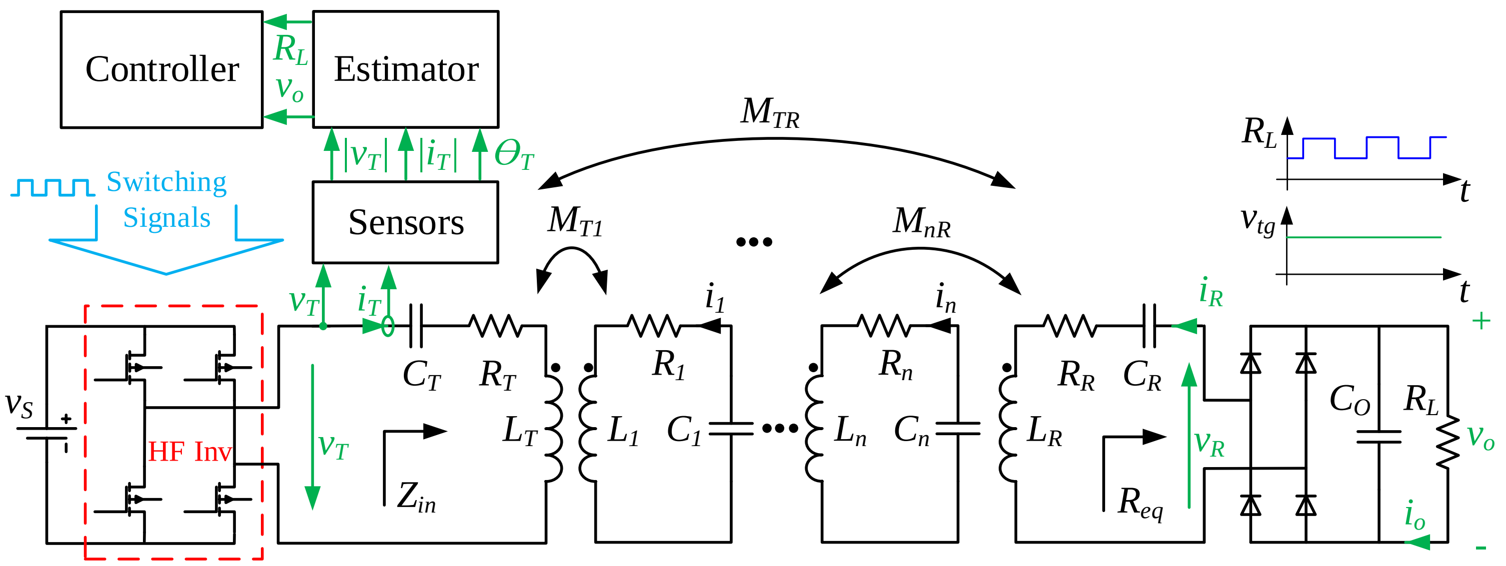

Schematic of a multi-coil WPT system in domino structure.

$$v_S H_1 \begin{bmatrix} 1 \\ 0 \\ \vdots \\ 0 \\ 0 \end{bmatrix} = \begin{bmatrix} R'_T & j\omega_s M_{T1} & \cdots & j\omega_s M_{TR} & 0 \\ j\omega_s M_{1T} & R'_1 & \cdots & j\omega_s M_{1R} & 0 \\ \vdots & \vdots & \ddots & \vdots & \vdots \\ j\omega_s M_{RT} & j\omega_s M_{R1} & \cdots & R'_R & 1 \\ 0 & 0 & \cdots & -8/\pi^2 & 1/R_L \end{bmatrix} \begin{bmatrix} I_T \\ I_1 \\ \vdots \\ I_R \\ H_2 v_o \end{bmatrix} + \begin{bmatrix} L'_T & M_{T1} & \cdots & M_{TR} & 0 \\ M_{1T} & L'_1 & \cdots & M_{1R} & 0 \\ \vdots & \vdots & \ddots & \vdots & \vdots \\ M_{RT} & M_{R1} & \cdots & L'_R & 0 \\ 0 & 0 & \cdots & 0 & C_o \end{bmatrix} \begin{bmatrix} \dot{I}_T \\ \dot{I}_1 \\ \vdots \\ \dot{I}_R \\ H_2 \dot{v}_o \end{bmatrix}$$

Experiment Setup

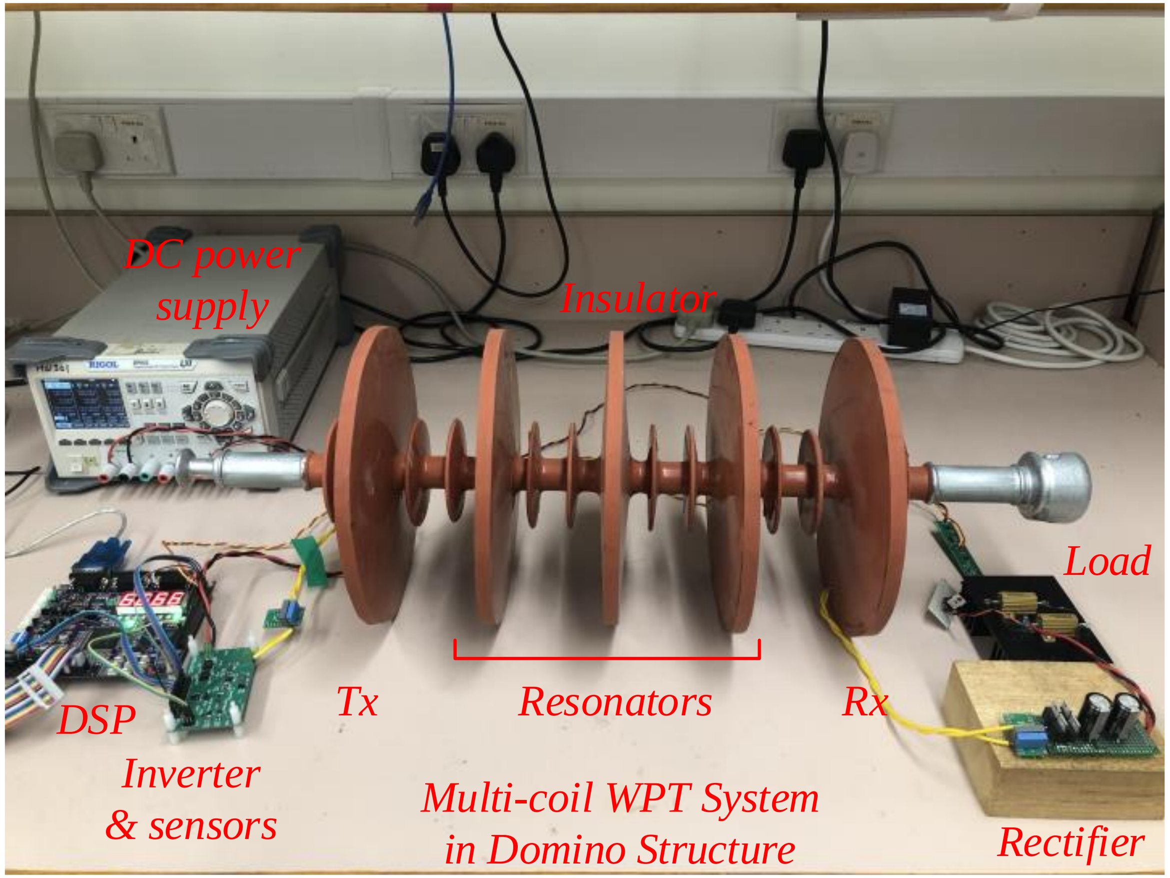

Experimental setups of the multi-coil WPT system in domino structure

Dynamic Load Identification Results

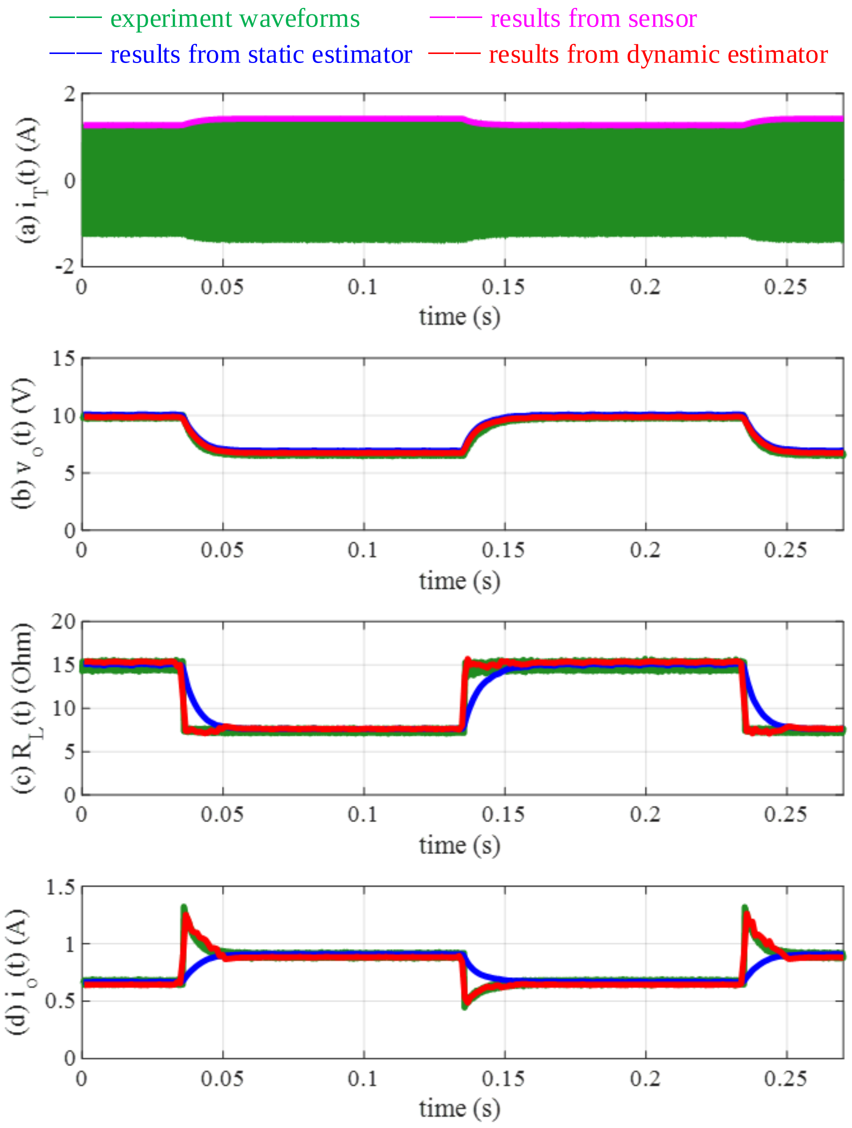

Experimental results when there are step changes on load resistance

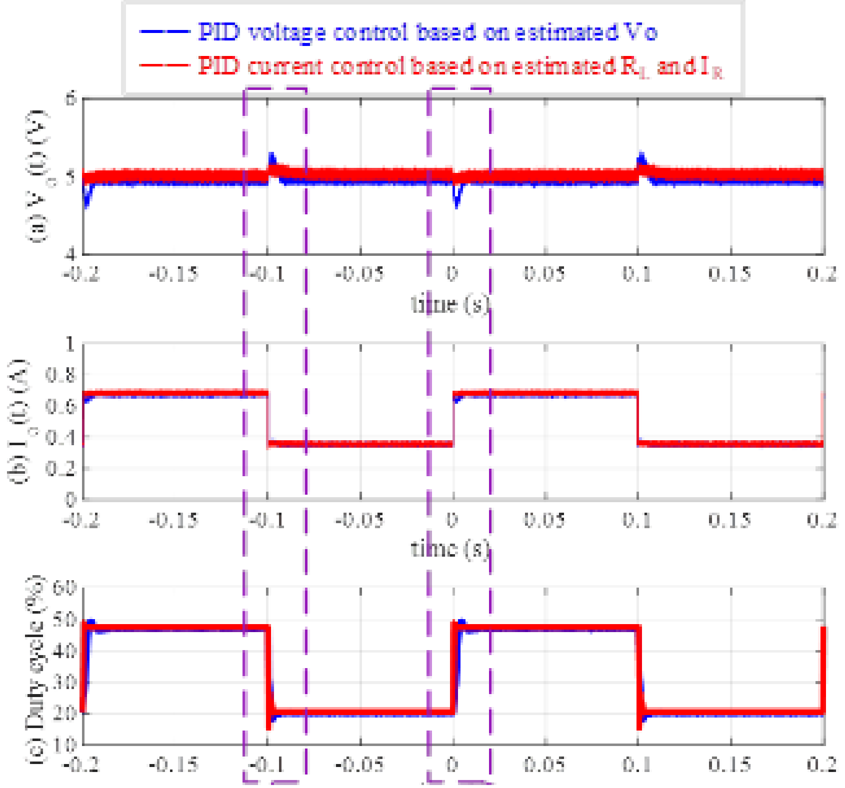

Transmitter side PID voltage control based on the dynamic estimator

Conclusions

- Identify two new challenges
  - Mid-range WPT for power grid monitoring equipment
  - Dynamic Modelling, load identification and Control
- Mid-range WPT system
  - Planar PCB resonant winding
  - Multi-coil WPT system over insulation distance
- Dynamic modelling
  - Phasor transformation for resonant circuit
  - Circuit model and equation model for WPT system
- New control method
  - Dynamic load identification using proposed model
  - Transmitter side control without wireless communication

Q&A